

# 第十二届“中国青少年科技创新奖” (申报材料)

学 校 宁夏医科大学

申 报 人 王国玮

联系电话 13519590119

邮 箱 wanguowei0119@163.com

申报日期 2020. 6. 23

## 目 录

一、奖学金	3
二、科技奖项	6
三、科研立项	7
四、发表论文	15

## 一、奖学金

- 1、2019 年硕士研究生国家奖学金
- 2、宁夏医科大学研究生学业二等奖学金（2017-2018）
- 3、宁夏医科大学研究生学业一等奖学金（2018-2019）



# 荣誉证书

王国玮同学

荣获 2017-2018 学年学校研究生二年级

学业奖学金二等奖。特发此证，以资鼓励。

宁夏医科大学  
二〇一八年十月



# 荣誉证书

王园玮同学：

荣获 2018-2019 学年学校研究生**三年级**

学业奖学金**一等奖**。特发此证，以资鼓励。

宁夏医科大学

二〇一九年十一月



## 二、科技奖项

1. 王振海, 杨晓军, **王国玮**, 刘爱翠, 刘强, 王妍柏, 汪超, 马巧丽, 赵春梅, 杨娟, 胡坤, 赵莉, 杨丽萍, 李芳。中枢神经系统感染脑脊液病原体检测及其可能损伤机制的系列研究, **宁夏科技进步二等奖(名次第三)**, 宁夏回族自治区人民政府, 2016.9.27



### 三、参与的科研项目

1. 2018 年宁夏科技重点（重大）研究计划：脑脊液细胞和分子诊断新技术开发和应用，（编号：2018BFG02017，经费 547 万元，项目组成员，在研）
2. 2019 年国家自然科学地区基金项目：“流行性乙型脑炎周围神经损害的关键蛋白筛选及其致病机制”（编号：81960233；经费：33.7 万元，项目组成员，在研）。
3. 2019 年宁夏科技重点（重大）研究计划：“流行性乙型脑炎病原体、发病机制及防控研究”，（编号：2019BCG01003，经费 375 万元，项目组成员，在研）。

## 国家自然科学基金资助项目批准通知

王振海 先生/女士：

根据《国家自然科学基金条例》和专家评审意见，国家自然科学基金委员会（以下简称自然科学基金委）决定批准资助您的申请项目。项目批准号：81960233，项目名称：流行性乙型脑炎周围神经损害的关键蛋白筛选及其致病机制，直接费用：33.70万元，项目起止年月：2020年01月至2023年12月，有关项目的评审意见及修改意见附后。

请尽早登录科学基金网络信息系统（<https://isisn.nsf.gov.cn>），获取《国家自然科学基金资助项目计划书》（以下简称计划书）并按要求填写。对于有修改意见的项目，请按修改意见及时调整计划书相关内容；如对修改意见有异议，须在电子版计划书报送截止日期前向相关科学处提出。

电子版计划书通过科学基金网络信息系统（<https://isisn.nsf.gov.cn>）上传，依托单位审核后提交至自然科学基金委进行审核。审核未通过者，返回修改后再行提交；审核通过者，打印纸质版计划书（一式两份，双面打印），依托单位审核并加盖单位公章后报送至自然科学基金委项目材料接收工作组。电子版和纸质版计划书内容应当保证一致。向自然科学基金委提交和报送计划书截止时间节点如下：

1. 提交电子版计划书截止时间为**2019年9月11日16点**（视为计划书正式提交时间）；
2. 提交电子修改版计划书截止时间为**2019年9月18日16点**；
3. 报送纸质版计划书截止时间为**2019年9月26日16点**。

**请按照以上规定及时提交电子版计划书，并报送纸质版计划书，未说明理由且逾期不报计划书者，视为自动放弃接受资助。**

附件：项目评审意见及修改意见表

国家自然科学基金委员会  
2019年8月16日





申请代码	H0909
接收部门	
收件日期	
接收编号	8196050488



8196050488

# 国家自然科学基金 申请书

(2019版)

资助类别: 地区科学基金项目

亚类说明:

附注说明:

项目名称: 流行性乙型脑炎周围神经损害的关键蛋白筛选及其致病机制

申请人: 王振海 电话: 0951-6744025

依托单位: 宁夏医科大学

通讯地址: 宁夏银川市兴庆区胜利街1160号

邮政编码: 750004 单位电话: 0951-6980063

电子邮箱: wangzhenhai1968@163.com

申报日期: 2019年02月19日

国家自然科学基金委员会

项目组主要参与者 (注: 项目组主要参与者不包括项目申请人)

编号	姓名	出生年月	性别	职称	学位	单位名称	电话	电子邮箱	证件号码	每年工作时间(月)
1	王钊	1988-11-04	男	博士生	硕士	宁夏医科大学	15209588305	wangzhaodoc88@163.com	1*****9	10
2	刘强	1983-10-25	男	副主任医师	硕士	宁夏医科大学	13519576006	liuqiang6006@163.com	6*****0	5
3	杨娟	1985-06-17	女	博士生	硕士	宁夏医科大学	13895643652	yangjuan7@163.com	6*****8	10
4	王妍柏	1983-08-01	女	主管技师	硕士	宁夏医科大学	15825310259	748913607@qq.com	2*****x	6
5	王国玮	1990-05-18	男	硕士生	学士	宁夏医科大学	13519590119	wangguowe10119@163.com	6*****3	10
6	余黎明	1992-10-02	男	博士生	硕士	宁夏医科大学	18595092098	1245292154@qq.com	4*****9	10
7	高鑫雷	1991-07-22	男	硕士生	学士	宁夏医科大学	18791128874	18791128874@163.com	6*****7	10
8	郭佳雨	1990-03-20	女	硕士生	学士	宁夏医科大学	15004322826	1203414531@qq.com	2*****1	10
9	贺茹	1991-11-08	女	硕士生	学士	宁夏医科大学	18809604102	2418321042@qq.com	6*****7	10

总人数		高级	中级	初级	博士后	博士生	硕士生
10		2	1			3	4

项目编号：2018BFG02017

# 宁夏回族自治区重点研发计划 重大（重点）项目任务书

项目名称：脑脊液细胞和分子诊断新技术开发和应用

项目牵头承担单位（公章）：宁夏医科大学总医院

项目合作单位（公章）：上海交通大学

项目合作单位（公章）：宁夏数据科技股份有限公司

项目负责人：王振海

项目归口管理单位（公章）：宁夏医科大学总医院

项目实施期：2018-10-01 至 2021-12-31

宁夏回族自治区科学技术厅

2018-07-27

## 九、研究人员基本情况

序号	姓名	性别	年龄	职称	学位	专业	为本项目工作时间 (%)	工作单位	签字
1	田永华	女	54	正高级	学士	内科学	40.0	宁夏医科大学总医院	
2	王士林	男	39	正高级	博士	电脑工程	60.0	上海交通大学网络安全工程学院	
3	马晓峰	男	41	正高级	博士	计算机科学与技术	60.0	宁夏数据科技股份有限公司	
4	王立斌	男	42	副高级	博士	生物化学与分子生物学	60.0	宁夏医科大学总医院	
5	安少荣	男	46	正高级	学士	通讯工程	40.0	宁夏建工集团有限公司	
6	黄琦	女	33	中级	硕士	生物化学与分子生物学	60.0	宁夏医科大学总医院	
7	侯玉婷	女	30	初级	硕士	医学检验	60.0	宁夏医科大学总医院	
8	王国玮	男	28	初级	硕士	神经病学	80.0	宁夏医科大学研究生院	
9	杨笑	女	42	正高级	博士	神经病学	50.0	宁夏医科大学总医院	
10	侯晓霖	男	41	副高级	硕士	神经病学	50.0	宁夏医科大学总医院	
11	李海宁	女	42	正高级	博士	神经病学	50.0	宁夏医科大学总医院	

项目编号：2019BCG01003

## 宁夏回族自治区重点研发计划 重大（重点）项目任务书

项目名称：宁夏地区流行性乙型脑炎病原学、致病机制  
和防控研究

---

承担单位：宁夏医科大学总医院（公章）

---

承担单位：中国疾病预防控制中心病毒病预  
防控制所（公章）

---

项目负责人：王振海

---

归口管理单位：宁夏医科大学（公章）

---

项目实施期：2019年12月至2022年12月

---

宁夏回族自治区科学技术厅

2019年11月12日

## 九、研究人员基本情况

序号	姓名	性别	年龄	职称	学位	专业	工作时间 (%)	工作单位	签字
1	王环宇	男	46	正高级	博士	病原生物学	50.0	中国疾病预防控制中心病毒病预防控制研究所	
2	杨晓军	女	51	正高级	硕士	重症医学	50.0	宁夏医科大学总医院	
3	李海宁	女	43	正高级	博士	神经病学	50.0	宁夏医科大学总医院	
4	郭涛	女	49	正高级	硕士	神经病学	33.0	宁夏医科大学总医院	
5	王钊	男	30	初级	硕士	神经病学	66.6	宁夏医科大学临床医学院	
6	王国玮	男	29	初级	学士	神经病学	88.9	宁夏医科大学临床医学院	
7	李樊	女	36	中级	博士	病原生物学	88.9	中国疾病预防控制中心病毒病预防控制研究所	
8	付士红	女	52	正高级	硕士	病原生物学	30.0	中国疾病预防控制中心病毒病预防控制所	

#### 四、发表或录用学术论文

在国际 SCI 期刊共发表或录用学术论文 4 篇。其中在《The New England Journal of Medicine》2020.6.9 录用 1 篇：

1. **Guowei Wang\***, Haining Li, Xiaojun Yang., Tao Guo, Libin Wang, Zhijun Zhao ,Haifeng Sun, Xiangchun Ding, Qiaoli Ma, Yanbo Wang, Zhenhai Wang \*, Huanyu Wang\*, Peng Xie\*, Guillain-Barré Syndrome Outbreak Associated with JEV Infection in China. **The New England Journal of Medicine. (Accepted, IF: 74.699)**

2.Li-Ning Yang\*, Jun-Cai Pu\*, Lan-Xiang Liu\*, **Guo-Wei Wang\***, Xin-Yu Zhou, Yu-Qing Zhang, Yi-Yun Liu, Peng Xie, Integrated Metabolomics and Proteomics Analysis Revealed Second Messenger System Disturbance in Hippocampus of Chronic Social Defeat Stress Rat. **Front Neurosci.** 2019; 13: 247. Published online 2019 Mar 22. doi: 10.3389/fnins.2019.00247 (**\*co-author, IF: 3.648**)

3.Luxuan Wang\*, **Guowei Wang\***, Yangyang Duan, Haining Li, et al. A comparative study of the diagnostic potential of plasma and erythrocytic  $\alpha$ -synuclein Parkinson's diseases. **Neurodegenerative Diseases**, 2020, 19(5-6):204-210. (**\*co-author, IF: 2.798**)

4. Juan Yang\*, **Guowei Wang\***, Haining Li\*, Wenli Zheng ,Burui Guo, Zhenhai Wang, Knockdown of Mg<sup>2+</sup>/Mn<sup>2+</sup>-dependent protein phosphatase 1A promotes apoptosis in microglia BV2 cells with Brucella suis vaccine strain2 infection. **Experimental and Therapeutic Medicines**, May 13, 2020, 926-932 (**\*co-author, IF:1.449**)

## 论文检索报告

委托内容： 王国玮的论文录用情况

委托单位： 宁夏医科大学

检索单位： 宁夏医科大学图书馆

完成日期： 2020年6月18日

宁夏医科大学图书馆

二〇一九年制



### 一、检索要求

- 1、被检作者：王国玮
- 2、委托单位：宁夏医科大学
- 3、论文发表年限：2020年
- 4、论文篇数：1篇

### 二、检索文献信息

序号	文献题名	署名情况	刊物名称	成果类别	发表年月
1	Guillain-Barré Syndrome Outbreak Associated with JEV Infection in China	第一作者	The New England Journal of Medicine	SCI, IF: 70.67	Accepted, 2020.6.9

### 三、检索结果

录用：

- 王国玮为第一作者发表文献，有1篇。（记录见附件1）

提供文献共计1篇，2019年12月26日在The New England journal of medicine/New Eng J Med投稿，于2020年6月9日被该杂志接收录用，尚未见刊，待刊出。（详细信息见附件2）

检索报告人：徐海荣

审核人：王见芳

检索单位：

宁夏医科大学图书馆

完成时间：

2020年6月18日



Please review the Supplemental Files folder to review documents not compiled in the PDF.

### Guillain-Barré Syndrome Outbreak Associated with JEV Infection in China

Journal:	<i>New England Journal of Medicine</i>
Manuscript ID	19-16977
Article Type:	Letter NOT about NEJM Article
Date Submitted by the Author:	26-Dec-2019
Complete List of Authors:	<p>Wang, Guowei; Ningxia Medical University, School of Clinical Medicine  Li, Haining; Ningxia Medical University, General Hospital of Ningxia Medical University, Neurology Center  Yang, Xiao; Ningxia Medical University, Neurology Center, General Hospital of Ningxia Medical University  Guo, Tao; Ningxia Medical University, General Hospital of Ningxia Medical University, Neurology Center;  Wang, Libin; Ningxia Medical University, General Hospital of Ningxia Medical University, Biochip research Center  Zhao, Zhijun; Ningxia Medical University, Ningxia Key Laboratory of Clinical and Pathogenic Microbiology; Clinical Laboratory Center, General Hospital of Ningxia Medicine Center  Sun, Haifeng; Ningxia Medical University, General Hospital of Ningxia Medical University, Neurology Center  Hou, Xiaolin; Ningxia Medical University, General Hospital of Ningxia Medical University, Neurology Center  Ding, Xiangchun; Ningxia Medical University, General Hospital of Ningxia Medical University, Department of Infectious Diseases  Dou, Chunyang; Ningxia Medical University, General Hospital of Ning Xia Medical University;  Ma, Qiaoli; Ningxia Medical University, General Hospital of Ningxia Medical University, Neurology Center  Yang, Xiaojun; Ningxia Medical University, General Hospital of Ningxia Medical University, Intensive Care Unit  Wang, Yanbo; Ningxia Medical University, General Hospital of Ningxia Medical University, Cerebrospinal Fluid Laboratory  Wang, Zhao; Ningxia Medical University, General Hospital of Ningxia Medical University, School of Clinical Medicine  Wang, Luxuan; Ningxia Medical University, School of Clinical Medicine  Liu, Jixiang; Ningxia Medical University, Ningxia Centers for Disease Control and Prevention ;  Wang, Zhenhai; Ningxia Medical University, General Hospital of Ningxia Medical University, Neurology Center ; Ningxia Medical University, Key Laboratory of Brain Diseases of Ningxia  Wang, Huanyu; National Institute for Viral Disease Control and Prevention, Department of Arbovirus  Xie, Peng; Chongqing Medical University First Affiliated Hospital, NHC Key Laboratory of Diagnosis and Treatment on Brain Functional Diseases; Chongqing Medical University First Affiliated Hospital</p>

Confidential: Destroy when review is complete.

### Guillain-Barré Syndrome Outbreak Associated with JEV Infection in China

To the Editor: This is the first study to document a large series of patients who developed Guillain-Barré syndrome (GBS) following Japanese encephalitis virus (JEV) infection.

JEV is a single stranded RNA virus transmitted by mosquitoes, the first case of Japanese encephalitis was reported in China in 1940.<sup>1</sup> From 2003 to 2018, China had reported 51,013 cases, including 173 cases in Ningxia. From July to September 2018, the largest outbreak of JEV infection occurred in the north of Ningxia, clusters of cases of the GBS were observed. A total of 289 suspected cases of JEV infection, 161 patients were confirmed with JEV infection through virus isolation, immunoassay in blood and cerebrospinal fluid (CSF), and were evaluated electrophysiologically and clinically. 38 (81%) patients had the presence of albuminocytologic dissociation in the CSF. The electromyography of 47 patients with JEV infection were consistent with GBS, and were classified into 4 (9%) cases of acute inflammatory demyelinating polyneuropathy, 22 (47%) cases of acute motor axonal neuropathy, 18 (38%) cases of acute motor-sensory axonal neuropathy (AMSAN), and 3 (6%) cases of acute sensory neuropathy. These patients had symptoms compatible with JEV infection before the onset of GBS, and met the GBS diagnostic criteria of Brighton.<sup>2</sup> A virus strain isolated from CSF of patients with GBS was identified as JEV genotype I by whole-gene sequencing. Sural nerve biopsies in 2 patients with AMSAN revealed axons and myelin damage. In the serum of 40 patients with GBS, 12 (30%) patients had an anti-glycaemic autoimmune response, mainly GM1, GM2, GD1a and GD1b, but 13 patients had received treatment

1  
2  
3  
4 with gamma globulin at least 3 day before. 28 (60%) patients with GBS received  
5  
6 intravenous immunoglobulin within two weeks of onset, 15 (54%) patients showed  
7  
8 significant improvement in symptoms and signs after one week of this treatment. In  
9  
10 July 2019, 17 patients were followed up 8 months after discharge with partial limb  
11  
12 weakness (47%), limb muscle atrophy (23%) and gaitism (12%) (Fig.1 and see the  
13  
14 Supplementary Appendix).  
15  
16  
17  
18

19  
20 In summary, more and more studies have reported the occurrence of GBS associated  
21  
22 with Zika virus (ZIKV).<sup>3,4</sup> However, only few cases of GBS with JEV infection have  
23  
24 been reported.<sup>5</sup> The causal link of JEV infection with GBS has supported by the fact  
25  
26 that a shorter latency (median 5 days) from the occurrence of JEV infection to the  
27  
28 development of GBS has been observed. Therefore, this study provides evidence for  
29  
30 the relationship between JEV infection and GBS.  
31  
32  
33

34  
35 Guowei Wang, M.S.

36  
37 School of Clinical Medicine, Ningxia Medical University, Yinchuan, China.

38  
39 Haining Li, M.D., Ph.D.

40  
41 Xiaojun Yang, M.D.

42  
43 Tao Guo, M.D.

44  
45 Libin Wang, Ph.D.

46  
47 Zhijun Zhao, Ph.D.

48  
49 Haifeng Sun, M.D.

50  
51 Xiaolin Hou, M.D.

52  
53 Xiangchun Ding, M.D.  
54  
55  
56  
57  
58  
59  
60

1  
2  
3  
4  
5  
6  
7  
8  
9  
10  
11  
12  
13  
14  
15  
16  
17  
18  
19  
20  
21  
22  
23  
24  
25  
26  
27  
28  
29  
30  
31  
32  
33  
34  
35  
36  
37  
38  
39  
40  
41  
42  
43  
44  
45  
46  
47  
48  
49  
50  
51  
52  
53  
54  
55  
56  
57  
58  
59  
60

Chunyang Dou, M.D.

Qiaoli Ma, M.D.

Xiao Yang, M.D.

Yanbo Wang, M.D.

General Hospital of Ningxia Medical University, Yinchuan, China.

Zhao Wang, M.S.

Luxuan Wang, M.S.

School of Clinical Medicine, Ningxia Medical University, Yinchuan, China.

Jixiang Liu, Ph.D.

Ningxia Center for Disease Control and Prevention, Yinchuan, China.

Zhenhai Wang, M.D., Ph.D.

Neurology Center, General Hospital of Ningxia Medical University, Yinchuan, China.

wangzhenhai1968@163.com.

Huanyu Wang, Ph.D.

Department of arbovirus, National Institute for Viral Disease Control and Prevention,

Chinese Center for Disease Control and Prevention. State Key Laboratory for Infectious

Disease Prevention and Control, Chinese Center for Disease Control and Prevention,

Beijing, China.

wanghy@ivdc.chinacdc.cn.

Peng Xie, M.D.

NHC Key Laboratory of Diagnosis and Treatment on Brain Functional Diseases, The

First Affiliated Hospital of Chongqing Medical University, Chongqing, China.

1  
2  
3  
4  
5  
6  
7  
8  
9  
10  
11  
12  
13  
14  
15  
16  
17  
18  
19  
20  
21  
22  
23  
24  
25  
26  
27  
28  
29  
30  
31  
32  
33  
34  
35  
36  
37  
38  
39  
40  
41  
42  
43  
44  
45  
46  
47  
48  
49  
50  
51  
52  
53  
54  
55  
56  
57  
58  
59  
60

xiepeng58@21cn.com.

Drs. Guowei Wang, Prof. Zhenhai Wang, Prof. Peng Xie and Prof. Huanyu Wang contributed equally to this letter.

We declare no competing interests. Prof. Zhenhai Wang as first corresponding author had full access to all the data in the study, and had final responsibility for the decision to submit the publication.

Supported by grants from the Science and Technology Key Research Program of Ningxia, China (2018BFG02017 and 2019BCG01003) and the National Natural Science Foundation of China (81960233 and 31660030).

1. Wang H, Liang G, Epidemiology of Japanese encephalitis: past, present, and future prospects, *Ther Clin Risk Manag*. 2015; 11: 435–448.
2. Fokke C, van den Berg B, Drenthen J, Walgaard C, van Doorn PA, Jacobs BC. Diagnosis of Guillain- Barré syndrome and validation of Brighton criteria. *Brain*. 2014 Jan; 137 (Pt 1): 33-43.
3. Parra B, Lizarazo J, Jiménez-Arango JA, et al. Guillain-Barré Syndrome Associated with Zika Virus Infection in Colombia. *N Engl J Med*. 2016 Oct 20; 375(16):1513-1523.
4. VM Cao-Lormeau, A Blake, S Mons, S Lastere, C Roche, et al. Ghawché, Guillain-Barré Syndrome outbreak caused by ZIKA virus infection in French Polynesia, *Lancet*. 2016 Apr 9; 387 (10027): 1531–1539
5. Xiang JY , Zhang YH , Tan ZR , Huang J , Zhao YW, Guillain-Barré syndrome associated with Japanese encephalitis virus infection in China. *Viral Immunol* 2014 Oct; 27 (8): 418-20.

Confidential: Destroy when review is complete.

## Table of the letter

Table 1. Clinical findings and lab results of patients with GBS\* (n=47)

Characteristics	n (%)	M(IQR)
Age (years)		59 (24-63)
Male	26 (55)	
JEV vaccination history	2 (4)	
Fever	47 (100)	
Headache	47 (100)	
Flaccid paralysis	36 (76)	
Areflexia or decreased reflexes	32 (68)	
Paresthesia	21 (44)	
Trouble breathing	44 (94)	
Disturbance of consciousness	39 (83)	
Time from JEV infection to onset symptoms of GBS <sup>†</sup> , day		5 (3-9)
<b>Results of CSF analysis</b>		
Proteins (g/L)		0.82 (0.45-1.82)
Increased CSF protein (cut-off: 0.55 g/L)	38 (81)	
Median white-cell count — Cells (/mm <sup>3</sup> )		5 (2-13)
<b>Pathogen detection</b>		
JEV-IgM were detected in serum, n (%)	47 (100)	
JEV-IgM were detected in CSF, n (%)	47 (100)	
JEV strain was isolated from serum, n (%)	0 (0)	
JEV strain was isolated from CSF, n (%)	1 (2)	
<b>Anti-glycolipids IgM were detected in serum and CSF of patients by enzyme immunodot, n<sub>serum</sub> (%) / n<sub>CSF</sub> (%)</b>		
Anti-glycolipids IgM (+) in Serum, n (%)	12 (30)	
Anti-GM1 IgM (+) in Serum, n (%)	7 (18)	
Anti-GM2 IgM (+) in Serum, n (%)	7 (18)	
Anti-GD1a IgM (+) in Serum, n (%)	3 (8)	
Anti-GD1b IgM (+) in Serum, n (%)	3 (8)	
Anti-glycolipids (GM1) IgM (+) in CSF, n (%)	1 (3)	
<b>Neurologic diagnosis, n (%) †</b>		
GBS Brighton criteria level 1	35 (74)	
GBS Brighton criteria level 2	8 (17)	
GBS Brighton criteria level 3	4 (9)	
<b>Results of nerve-conduction studies and EMG, n (%)</b>		
AIDP	4 (9)	
AMSAN	18 (38)	
AMAN	22 (47)	
ASN	3 (6)	
<b>Treatment</b>		
Glucocorticoid	47 (100)	
Intravenous immune globulins	28 (60)	
Patients admitted to intensive care	44 (94)	
Required mechanical ventilation — n (%)	44 (94)	
Patients with GBS were followed up after 8 months	17 (36)	

Confidential: Destroy when review is complete.

1  
2  
3  
4  
5  
6  
7  
8  
9  
10  
11  
12  
13  
14  
15  
16  
17  
18  
19  
20  
21  
22  
23  
24  
25  
26  
27  
28  
29  
30  
31  
32  
33  
34  
35  
36  
37  
38  
39  
40  
41  
42  
43  
44  
45  
46  
47  
48  
49  
50  
51  
52

Muscle weakness	8 (47)
Incapacity to walk	7 (41)
Muscle atrophy	4 (23)
Incontinence	5 (29)
Hoarse voice	2 (11)

**Notes:** \*GBS, Guillain–Barré syndrome. AIDP, acute inflammatory demyelinating polyneuropathy. AMAN, acute motor axonal neuropathy. AMSAM, acute motor-sensory axonal neuropathy. ASN, acute sensory neuropathy. CSF, cerebrospinal fluid. EMG, electromyography. †The onset of neurologic symptoms was defined as the first day of onset of limb weakness, sensory symptoms, facial paralysis, or other neurologic symptoms. ‡Brighton criteria levels indicate the certainty of a diagnosis of the Guillain–Barré syndrome. Level 1 diagnosis is supported by nerve-conduction studies and the presence of albuminocytologic dissociation in the CSF. Level 2 diagnosis is supported by either a CSF white-cell count of less than 50 cells per cubic millimeter (with or without an elevated protein level) or nerve-conduction studies consistent with the Guillain–Barré syndrome, if the CSF white-cell count is unavailable). Level 3 diagnosis is based on clinical features without support from nerve-conduction or CSF studies.

Table 1 shows the clinical findings, diagnosis and treatment, and laboratory test results of patients with Guillain–Barré syndrome. Particularly, one JEV strain was isolated from cerebrospinal fluid in patient, it was identified as JEV 1 b.



New England Journal of Medicine 19-16977

发件人: NEJM Letter<onbehalf@manuscriptcentral.com> (由 010101729a45096d-42def8e8-860f-433f-b0b8-8897aa6220d0-000000@outbound)

收件人: 王国玮<wangguowei0119@163.com> 李海宁<lhnwww@126.com> cckk606@sina.com<cckk606@sina.com> 郭涛-神内<zfgt1@163.com>

时间: 2020年06月10日 02:08 (星期三)

附件: 4个 (PDF\_NEJM-CTA-2017-LTE.pdf等) 查看附件

你可以用泛微OA流程审批、合同管理... 在线试用>>

翻译成中文

Dear Prof. Wang,

I am pleased to inform you that your Letter to the Editor entitled, "Guillain-Barré Syndrome Outbreak Associated with JEV Infection in China," has been accepted for publication in the June 11, 2020 issue of the New England Journal of Medicine.

Acceptance for publication is made with the understanding that the material in your letter has not been published previously. In the exercise of the discretion of the editors, the letter will appear in print, online at NEJM.org, or both.

There should be no announcements or news releases about your letter until the day before the date of publication.

You should inform us immediately if you or any co-authors have any financial relationships with any company whose products are mentioned in your letter. Each author must complete one. For physicians practicing in the United States, please ensure that all relevant payor information (https://openpaymentsdata.cms.gov/search/physicians/by-name-and-location) have been included on your form. For information on the disclosure form. After you have filled in the appropriate information in the spaces provided, you may either e-mail your completed form to the appropriate editor or return it to the editorial office. Please be aware that in the event of publication, each author's disclosure form will be posted online with the article as supplemental material.

Each author must also sign and return the attached Copyright Transfer Agreement form via fax to 617-830-8135. Please note that the signed copyright agreements from all authors within 72 hours of receipt.

# Manuscripts with Decisions

ACTION	STATUS	ID	TITLE
Copyright Completion - No Ref Letter submitted (11-Jun-2020) - <a href="#">view</a>	Accepted (09-Jun-2020)	19-16977	Guillain-Barré Syndrome Outbreak Associated with JEV Infection in China <a href="#">View Submission</a>
Disclosure Completion - No Ref Letter submitted (11-Jun-2020) - <a href="#">view</a>	Decision Letter Pending		
	<a href="#">view decision letter</a>		

Dear Letter (19-16977)

From: letter@nejm.org

To: wangqunwei0119@163.com, 8nwww@126.com, cck6606@china.com, zfg1@163.com, wanglibin007@126.com, 2158151@163.com, Sushf3010@126.com, 13995381963@163.com, dengguangchun@nyfy.com.cn, douchunyang@126.com, maqiao666@163.com, yxjcu@163.com, 748913607@qq.com, 1031430549@qq.com, luxuanW@aliyun.com, jjsb100@163.com, 13995089189@163.com, wanghy@wdc.chinacdc.cn, xiepeng58@21cn.com

CC:

Subject: New England Journal of Medicine 19-16977

Body: Dear Prof. Wang,

I am pleased to inform you that your Letter to the Editor entitled, "Guillain-Barré Syndrome Outbreak Associated with JEV Infection in China," has been accepted for publication in edited form in a forthcoming issue of the Journal.

Acceptance for publication is made with the understanding that the material in your letter has not been published previously and will not be submitted for publication elsewhere before it appears in the Journal. At the discretion of the editors, the letter will appear in print, on NEJM.org, or both.

There should be no announcements or news releases about your letter until the day before the date of publication.

You should inform us immediately if you or any co-authors have any financial relationships with any company whose products are mentioned in the letter or a company making a competing product. A Universal Disclosure Form is attached. Each author must complete one. If practicing in the United States, please ensure that all relevant payments listed in the Open Payments database (available for review at <https://openpaymentsdata.cms.gov/search/physicians/?v=name-and-location>) have been included on your form. For information on what a "relevant" disclosure, please review the instructions on page 1 of your disclosure form. After you have filled in the appropriate information in the spaces provided, you may either e-mail your completed form to [letter@nejm.org](mailto:letter@nejm.org) or upload it to your Author Dashboard of 5d Manuscripts. Please be aware that in the event of publication, each author's disclosure form will be posted online with the article as supplemental material (with all dollar amounts redacted).

Each author must also sign and return the attached Copyright Transfer Agreement form via fax to 617-830-8125. Please note that we require handwritten signatures on this form. This acceptance is contingent upon our receiving the signed copyright agreements from all authors within 48 hours of receipt.

The Journal will edit your letter in accordance with its established style. You will receive a proof of the edited letter by e-mail; the proof stage will be your next opportunity to make changes. For important information about production and proofs, see the attached document. If you have any questions about these policies, you should call to discuss them.

Thank you for your submission, and for your interest in the Journal.

Sincerely,

Edward W. Campion, M.D.  
Executive Editor  
New England Journal of Medicine  
[617-734-9800; [ecampion@nejm.org](mailto:ecampion@nejm.org)]

New England Journal of Medicine  
10 Shattuck Street  
Boston, MA 02115  
(617) 734-9800  
Fax: (617) 739-9854  
<http://www.nejm.org>

Sent: 09-Jun-2020

File 1: "NEJM-CTA-2017-LTE.pdf"

File 2: "NEJM-ICMJE-2013.pdf"

File 3: "NEJM-LTE-inst-for-ICMJE-form-S-12.pdf"

File 4: "Production-and-proof.pdf"

7/15/2020 11:03:13 AM

# Integrated Metabolomics and Proteomics Analysis Revealed Second Messenger System Disturbance in Hippocampus of Chronic Social Defeat Stress Rat

Li-Ning Yang<sup>1,2†</sup>, Jun-Cai Pu<sup>1,2†</sup>, Lan-Xiang Liu<sup>1,2†</sup>, Guo-Wei Wang<sup>3†</sup>, Xin-Yu Zhou<sup>4</sup>, Yu-Qing Zhang<sup>5</sup>, Yi-Yun Liu<sup>1,2</sup> and Peng Xie<sup>1,2\*</sup>

<sup>1</sup> Department of Neurology, The First Affiliated Hospital of Chongqing Medical University, Chongqing, China, <sup>2</sup> Institute of Neuroscience and the Collaborative Innovation Center for Brain Science, Chongqing Medical University, Chongqing, China, <sup>3</sup> School of Clinical Medicine, Ningxia Medical University, Yinchuan, China, <sup>4</sup> Department of Psychiatry, The First Affiliated Hospital of Chongqing Medical University, Chongqing, China, <sup>5</sup> Department of Neurology, The Second Affiliated Hospital of Chongqing Medical University, Chongqing, China

## OPEN ACCESS

### Edited by:

Firas H. Kobeissy,  
University of Florida, United States

### Reviewed by:

Oksana Sorokina,  
University of Edinburgh,  
United Kingdom  
Ying Xu,  
University at Buffalo, United States

### \*Correspondence:

Peng Xie  
xiepeng@cqmu.edu.cn

<sup>†</sup>These authors have contributed  
equally to this work

### Specialty section:

This article was submitted to  
Systems Biology,  
a section of the journal  
Frontiers in Neuroscience

Received: 19 November 2018

Accepted: 01 March 2019

Published: 22 March 2019

### Citation:

Yang L-N, Pu J-C, Liu L-X,  
Wang G-W, Zhou X-Y, Zhang Y-Q,  
Liu Y-Y and Xie P (2019) Integrated  
Metabolomics and Proteomics  
Analysis Revealed Second Messenger  
System Disturbance in Hippocampus  
of Chronic Social Defeat Stress Rat.  
Front. Neurosci. 13:247.  
doi: 10.3389/fnins.2019.00247

Depression is a common and disabling mental disorder characterized by high disability and mortality, but its physiopathology remains unclear. In this study, we combined a non-targeted gas chromatography-mass spectrometry (GC-MS)-based metabolomic approach and isobaric tags for relative and absolute quantitation (iTRAQ)-based proteomic analysis to elucidate metabolite and protein alterations in the hippocampus of rat after chronic social defeat stress (CSDS), an extensively used animal model of depression. Ingenuity pathway analysis (IPA) was conducted to integrate underlying relationships among differentially expressed metabolites and proteins. Twenty-five significantly different expressed metabolites and 234 differentially expressed proteins were identified between CSDS and control groups. IPA canonical pathways and network analyses revealed that intracellular second messenger/signal transduction cascades were most significantly altered in the hippocampus of CSDS rats, including cyclic adenosine monophosphate (cAMP), phosphoinositid, tyrosine kinase, and arachidonic acid systems. These results provide a better understanding of biological mechanisms underlying depression, and may help identify potential targets for novel antidepressants.

**Keywords:** depression, social defeat, proteomics, metabolomics, second-messenger

**Abbreviations:** AA, arachidonic acid; cAMP, cyclic adenosine monophosphate; CON, non-stress control; CSDS, chronic social defeat stress; EPM, elevated plus maze; FDR, false discovery rate; FST, forced swim test; GABA, 4-aminobutyric acid; GABA-T, 4-aminobutyrate aminotransferase; GC-MS, gas chromatography-mass spectrometry; GPCRs, G protein-coupled receptors; IPA, ingenuity pathway analysis; iTRAQ, isobaric tags for relative and absolute quantitation; LAT, locomotor activity test; LC-MS, liquid chromatography-mass spectrometry; LE, long-evans; MDD, major depressive disorder; NAA, N-acetyl-L-aspartic acid; NMR, nuclear magnetic resonance; OFT, open field test; OPLS-DA, orthogonal partial least-squares discriminant analysis; PCA, principal components analysis; PI3K, phosphoinositide-3-kinase; PKA, protein kinase A; PLD, phospholipase D; SD, sprague-dawley; SPT, sucrose preference test; VIP, variable importance on projection.

## INTRODUCTION

Depression is one of the most prevalent psychiatric and disability diseases conditions in the world today, but its physiopathology remains poorly elucidated (Health TNiOM, 2016; World Health Organization [WHO], 2017). Among various animal models, social defeat stress is one of the most widely used for investigating possible causes of and treatments for depression (Becker et al., 2008; Ota et al., 2014). Chronic social stress requires learned social defeat for a long period, usually combined with repeated exposure to sensory stimuli from aggressive rodents (Denmark et al., 2010). The repeated exposure of rodents to social defeat causes a solid depression-like behavior marked by anhedonia, body weight alteration, and altered protein expression in various brain areas (Vyas et al., 2002; Radley and Morrison, 2005; Denmark et al., 2010).

Hippocampus is a key brain area for emotion and motivation generation and regulation, and plays a critical influence in the etiology of depression (Campbell and Macqueen, 2004; McEwen et al., 2012). Neuropathological studies of hippocampus showed atrophy of hippocampal neurons (Sousa et al., 2000; Harrison, 2002; Lucassen et al., 2006; McEwen, 2010). However, how these changes in hippocampus lead to depression still unclear (Christoffel et al., 2011). Revealing these molecular events is essential for understanding the pathogenesis of depression.

In recent decades, omics technologies have become a powerful tool to uncover the physiopathology of neuropsychiatric disorders (Zheng et al., 2013a, 2016a; Zhou et al., 2015). Metabolomics can quantify low-molecular-weight metabolites in specific biological sample, and is widely used to capture disease-specific metabolite signatures (Lindon and Nicholson, 2008; Koike et al., 2014; Proitsi et al., 2015). Proteomics – the analysis of protein expression in biological samples – can provide insights into the pathophysiological mechanisms of several disease states (Taurines et al., 2011). Previously, our team completed a series of research on depression in clinical patients and animal models using a single omics technology (Zheng et al., 2013b, 2016b; Chen et al., 2015; Liu et al., 2016; Wang et al., 2016; Zhou et al., 2018). Recently, researchers have started to use combinatorial omics approaches to study the physiopathology of various diseases, including cancer, cardiovascular disease, and psychiatric disorders (Mayr et al., 2008; Ma et al., 2012; Wesseling et al., 2013). In those studies, metabolomics informed functional interpretations of proteomic results, and proteomics helped to a better understanding of metabolomics results by emphasizing the involvement of specific enzymatic and/or enzymatic pathways. With respect to depression, significantly perturbed energy metabolism in the cerebellum and dysfunction of amino acid metabolism and lipid metabolism in the hippocampus of chronically stressed rats has been observed, and disturbance of phospholipid metabolism in the plasma of MDD patients has been found in previous studies using integrated analysis of proteomic and metabolomic profiles (Shao et al., 2015; Gui et al., 2018; Zhang et al., 2018). Hence, combining proteomic analysis with metabolic profiling is promising and may help to elucidate complete biological mechanisms (Cavill et al., 2016).

The purpose of this research was to elucidate metabolite and protein alterations induced by depression in rat hippocampus after CSDS. We combined a non-targeted GC-MS-based metabolomic approaches with iTRAQ-based proteomic analysis. Furthermore, IPA was conducted to integrate potential relationships among altered metabolites and proteins to better understand the physiopathology of depression.

## MATERIALS AND METHODS

### Animals and Ethics Statement

This research (including stress and behavioral tests) was conducted in accordance with recommendations of the Guide for the Care and Use of Laboratory Animals, and approved by the Ethics Committee of Chongqing Medical University. All procedures contributing to this work comply with the ethical standards of the relevant national and institutional committees on animal experimentation. As described in our previous study, thirty-five male SD rats, 250–300 g, were kept in a separate cage as experimental intruder or control animals (Liu et al., 2018). Male LE rats, 380–450 g, were housed in pairs with ligatured female LEs served as resident rats. All animals lived under a 12-h day-and-night regime (lights on at 19:00) in controlled environmental conditions ( $21 \pm 1^\circ\text{C}$ ,  $55 \pm 5\%$  relative humidity) to ensure that all manipulations and tests were performed during the active phase (subjective night) of rats. Food and water were available *ad libitum*. Before starting the experimental procedures, all animals were adapted to light regime, controlled environmental conditions, as well as handling and presence of the experimenter in the room for 10 days.

Using measurements of body weight, sucrose preference, and activity, outliers at baseline were removed, leaving twenty-eight SD rats that were body weight matched and randomly divided into the CSDS group or CON group.

### Experimental Procedures

#### Social-Defeat Procedure

The social defeat pattern included two consecutive periods (a total 60 min) in LE rats' home cages. During period I (5 min), rats were allowed physical confrontation. In period I, when the interaction became too strong or once the SD rat surrendered or acquired a supine position over 5 seconds, the SD rat was transported to a small wire mesh protective cage (10 cm  $\times$  10 cm  $\times$  15 cm) within the LE's home and spend the remaining 60 min (period II). Hence, the wire mesh cage allowed for comprehensive visual, olfactory, as well as auditory exposure to LE rat without direct physical contact. CON group rats were placed in the empty LE rats' home cages for 60 min. The 60-min social defeat exposure was repeated once daily for 5 days during weeks 1 and 3, and once daily for 3 days during week 2. The overall experimental procedure is shown in Figure 1.

#### Behavioral Tests

Weight measurement and SPT were conducted at baseline and weekly during for 3 weeks. In addition, during the whole experiment, a series of behavioral tests were carried out in a

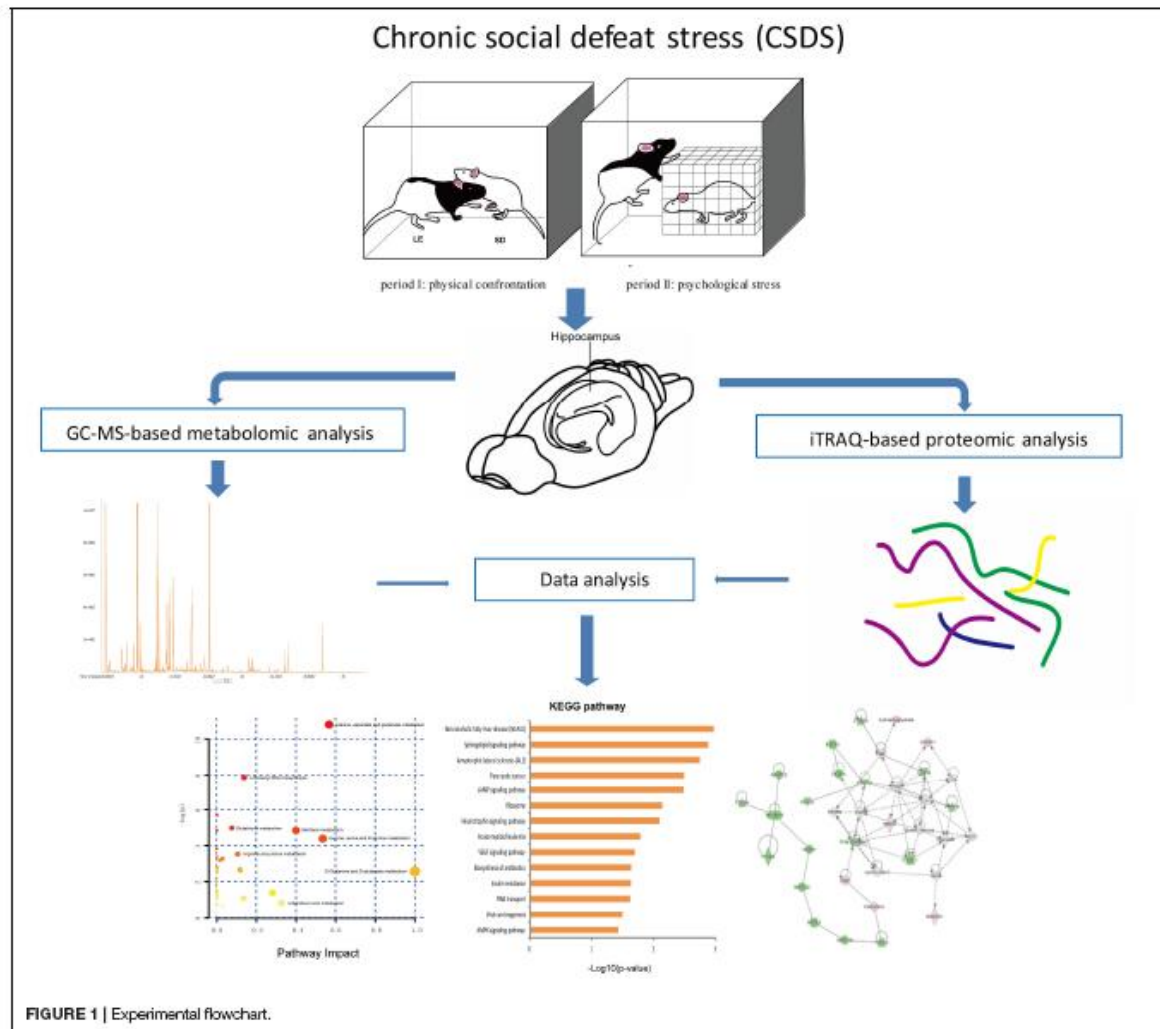
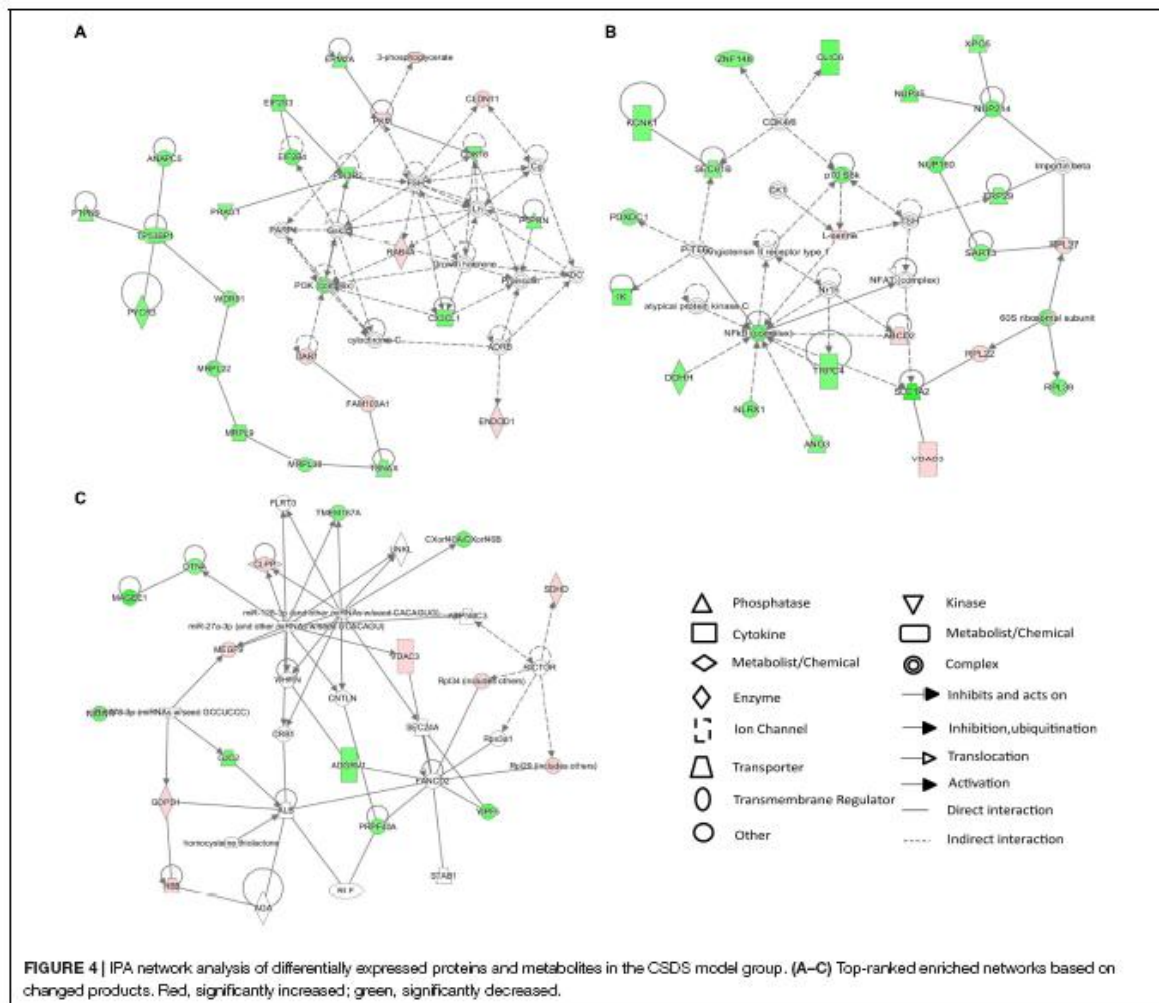


**Figure 2D.** Overviews of pathway and enrichment analyses based on metabolite alterations are displayed in **Figures 2E,F**.

### iTRAQ-Based Proteomic Analyses

Using iTRAQ-based proteomic profiling of hippocampus from CSDS and CON groups, 4950 proteins were detected with at least one unique peptide and a 1% FDR. A volcano plot of all proteins is displayed in **Figure 3A**. Based on the criteria mentioned above, 234 differentially expressed proteins were identified and chosen for further analysis between CSDS group and CON group (**Supplementary Table S2**). Among them, 66 proteins were increased and 168 were decreased expression. Heatmap visualization of 234 differentially expressed proteins is displayed in **Figure 3B**. As shown in the **Figure 3B**, CSDS group and CON group were clearly separated, and three replicates of each group showed good reproducibility. According to hierarchical

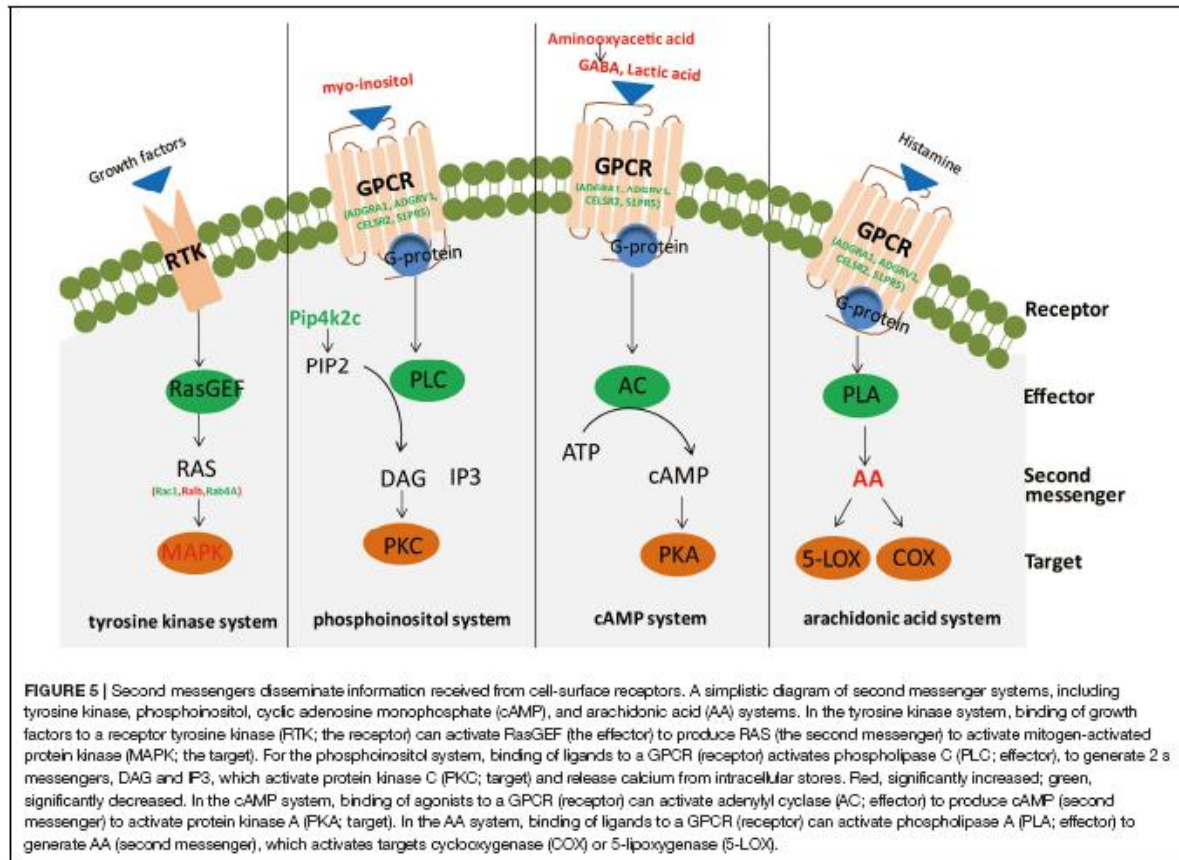
clustering analysis, proteins were resulted into three clusters. The proteins in cluster 1 were most associated with positive regulation of neuron death, while those in cluster 2 were most associated with translation, and those in cluster 3 were most associated with protein transport. Gene Ontology (GO) analysis annotated 221 proteins and then resulted them into 19 significant GO terms for biological processes (**Figure 3D**), 29 for cellular components (**Figure 3E**), and 14 for molecular function (**Figure 3F**). A total of 196 altered proteins were annotated by STRING. The Protein-Protein interaction (PPI) network of these proteins is showed in **Figure 3C**. The PPI network analysis revealed that MAP3K5, PIK3R2, RAC1, PIP4K2C, and PPP2R2B participated in various biological progress such as single-organism cellular process or single-organism transport, and MAP3K5, PIK3R2, RAC1, PIP4K2C, and BAD participated in neurotrophin signaling pathway, which may play a critical



associated with depression (Odagaki et al., 2001; Gould and Manji, 2002; Skelin et al., 2011; Niciu et al., 2013; Fujita et al., 2017). The cAMP second messenger system plays a pivotal role in neuroplasticity and depression; in addition, studies have shown that antidepressant treatment can alter the expression of components of this signaling pathway in rodents (Popoli et al., 2000; Fujita et al., 2017). In this research, we found that GABA, lactic acid, and aminoxyacetic acid were significantly elevated in the hippocampus. Among these three metabolites, GABA and lactic acid can participate in the cAMP signaling pathway through binding and activation of GPCRs, and aminoxyacetic acid can inhibit GABA-T activity, leading to a reduction of GABA breakdown (Wallach, 1961). Moreover, GPCRs (including ADGRA1, ADGRV1, CELSR2, and S1PR5) previously reported to be implicated in the physiopathology and pharmacology of depression were also significantly altered (Tomita et al., 2013). Whereas previous studies observed

decreased activation of adenylate cyclase and PKA in depression (Gould and Manji, 2002; Akin et al., 2005), in this study, we found a significant decrease of PPP1R13B and PPP2R2B, two phosphate family proteins that counterbalance the action of PKA (Fimia and Sassone-Corsi, 2001), in the hippocampus. Unexpectedly, but consistent with earlier researches, we did not observe changes in cAMP levels (Belmaker et al., 1980; Maj et al., 1984). However, changes in receptor-mediated cAMP formation have been studied in depression (Dwivedi and Pandey, 2008). These researches indicate PKA and associated cAMP signaling molecules may act as crucial neurobiological factors in depression (Dwivedi and Pandey, 2008).

Alterations of phosphoinositol signaling in the cerebra and peripheral tissues of depressed patients have been extensively reported, and studies have found that mood stabilizers (e.g., lithium, and valproate) seem to partially repair these abnormalities (Lenox et al., 1992; Kofman and Belmaker, 1993;



Yuan et al., 2001; Gould and Manji, 2002). In this study, significantly altered metabolites and proteins (including myo-inositol, PLD2, and PIP4K2C) involved in phosphoinositol second messenger systems were observed. Myo-inositol is a by-product of membrane-bound phospholipid metabolism and an important player in the phosphoinositide secondary messenger pathway (Yildiz-Yesiloglu and Ankerst, 2006). A previous study reported that elevated levels of myo-inositol could arise from disturbances in the coupling metabolism of the receptor-second messenger system complex, thus providing an important biological substrate for the onset of depression (Hemanth Kumar et al., 2012). Protein PIP4K2C may play a critical influence in the generation of phosphatidylinositol biphosphate, which is a precursor for second messengers of phosphoinositide signaling pathways (Itoh et al., 1998; Bulley et al., 2015). Meanwhile, PLD2 is an isoenzyme of PLD, which catalyzes the hydrolysis of phosphatidylcholine to generate an important lipid second messenger, phosphatidic acid (Kolesnikov et al., 2012; Zhu et al., 2018). These results are consistent with our previous plasma proteomic and metabolomic study, which found the dysregulation of phospholipid metabolism may aggravate inflammation in the central nervous system, ultimately leading to depression (Gui et al., 2018).

Small G proteins, which function as monomeric small GTPases, form one of the two classes of G proteins. In this study, elevated levels of three small GTPases, Rac1, RALB, and RAB4A, were observed. In addition, a significantly altered protein level of MAP3K5, a member of the MAP kinase kinase family and part of the mitogen-activated protein kinase pathway, was observed. These factors are reportedly involved in signal transduction as second messengers for the tyrosine kinase system. AA, a polyunsaturated fatty acid that plays an important role in regulating inflammation signals and (possibly) vulnerability to depression, participated in cellular signaling as a lipid second messenger (Janssen-Timmen et al., 1994; Lotrich et al., 2013; Newton et al., 2016).

Furthermore, there are other metabolites and proteins involved in second messenger systems, including serine, O-phosphorylethanolamine, NAA, and protein PIK3R2. Serine and O-phosphorylethanolamine are involved in sphingolipid metabolism and sphingolipid signaling. In recent studies, sphingolipids (more specifically ceramides) were proposed to act as lipid second messengers in intracellular signaling pathways and participate in the induction of apoptosis in many cells activated by GPCR or stress stimuli (Venkataraman and Futerman, 2000; Guzmán et al., 2001; Newton et al., 2016). Recent

reports suggest NAA is a main format of storage and transport of acetyl-coenzyme A in the neural system, where it is proposed to act as a second messenger relaying extracellular signals to the intracellular milieu (Ariyannur et al., 2010; Pietrocola et al., 2015). A recent research demonstrated that changes in the PI3K/AKT pathway may have specific therapeutic effects on depression (Kitagishi et al., 2012). In our study, we observed decreased PIK3R2, a regulatory subunit of PI3K, which belongs to the PI3K family. PI3Ks are enzymes that play an essential influence in lipid second messengers production and numerous biological reaction transduction.

There are some limitations of this study. First, the total number of included samples is relatively small, which may restrict interpretation of our results. Second, a number of low polarity metabolites are not detected by GC-MS. Therefore, GC-MS combined with other metabolomics approaches should be considered in future metabolomic studies. Third, iTRAQ and label-free, two quantitative proteomic analysis methods, have their own superiorities. The combination of these two methods can be complementary and should be considered in future studies. Fourth, proteomic results have not been validated by targeted methods. Thus, further researches are needed to validate these findings.

## CONCLUSION

In summary, we applied complementary omics strategies (GC-MS-based metabolomics and iTRAQ-based proteomics) to comprehensively elucidate metabolite and protein alterations in the hippocampus of rat after CSDS. The results of this study suggest that disturbances in several different secondary messenger systems (cAMP, phosphoinositol, AA, and tyrosine kinase) are involved in the hippocampus of CSDS rodents. An imbalance of second messengers may be related to the pathophysiology of depression. The results of our study contribute to a better understanding of biological mechanisms and pathophysiology of depression, and may contribute to identify novel targets for antidepressant treatment.

## REFERENCES

- Akin, D., Manier, D. H., Sanders-Bush, E., and Shelton, R. C. (2005). Signal transduction abnormalities in melancholic depression. *Int. J. Neuropsychopharmacol.* 8, 5–16. doi: 10.1017/s146114570400478x
- Ariyannur, P. S., Moffett, J. R., Manickam, P., Pattabiraman, N., Arun, P., Nitta, A., et al. (2010). Methamphetamine-induced neuronal protein NAT8L is the NAA biosynthetic enzyme: implications for specialized acetyl coenzyme A metabolism in the CNS. *Brain Res.* 1335, 1–13. doi: 10.1016/j.brainres.2010.04.008
- Autry, A. E., Adachi, M., Nosyreva, E., Na, E. S., Los, M. F., Cheng, P. F., et al. (2011). NMDA receptor blockade at rest triggers rapid behavioural antidepressant responses. *Nature* 475, 91–95. doi: 10.1038/nature10130
- Becker, C., Zeau, B., Rivat, C., Blugeot, A., Hamon, M., and Benoliel, J. J. (2008). Repeated social defeat-induced depression-like behavioral and biological alterations in rats: involvement of cholecystokinin. *Mol. Psychiatry* 13, 1079–1092. doi: 10.1038/sj.mp.4002097
- Belmaker, R. H., Zohar, J., and Ebstein, R. P. (1980). Cyclic nucleotides in mental disorder. *Adv. Cyclic Nucleotide Res.* 12, 187–198.

## AUTHOR CONTRIBUTIONS

L-NY and PX conceived and designed the study. L-NY, J-CP, L-XL, X-YZ, Y-QZ, and Y-YL collected the data. L-NY, J-CP, and L-XL analyzed the data. L-NY wrote the first draft of the manuscript. L-NY, G-WW, and PX interpreted the data and wrote the final version. All authors approved final version of the manuscript.

## FUNDING

This work was supported by the National Key Research and Development Program of China (Grant No. 2017YFA0505700), and the National Natural Science Foundation of China (Grant Nos. 8170051561 and 81873800). The funders had no role in the study design, data collection and analysis, decision to publish, or preparation of the manuscript.

## SUPPLEMENTARY MATERIAL

The Supplementary Material for this article can be found online at: <https://www.frontiersin.org/articles/10.3389/fnins.2019.00247/full#supplementary-material>

**FIGURE S1** | Results of Behavioral tests. (A) Body weight change between CSDS group ( $n = 9$ ) and CON group ( $n = 8$ ). (B) Sucrose preference changes between CSDS and CON groups. (C) Immobility time in the forced swim test. (D–F) Total distance, time spent in the inner squares, and rearing frequency in the open field test, respectively. (G–I) Open arms time, closed arms time, number of open arms entries, and number of closed arms entries in the elevated plus-maze, respectively. \* $P < 0.05$ .

**TABLE S1** | Identified differential metabolites in the hippocampus between the CSDS and CON groups.

**TABLE S2** | Identified differential proteins in hippocampus between the CSDS and CON groups.

**TABLE S3** | Top ten canonical pathways by IPA analysis of integrated data from proteomics and metabolomics.

- Bulley, S. J., Clarke, J. H., Droubi, A., Giudici, M. L., and Irvine, R. F. (2015). Exploring phosphatidylinositol 5-phosphate 4-kinase function. *Adv. Biol. Regul.* 57, 193–202. doi: 10.1016/j.jbior.2014.09.007
- Campbell, S., and Macqueen, G. (2004). The role of the hippocampus in the pathophysiology of major depression. *J. Psychiatry Neurosci.* 29, 417–426.
- Cavill, R., Jennen, D., Kleinjans, J., and Briede, J. J. (2016). Transcriptomic and metabolomic data integration. *Brief. Bioinform.* 17, 891–901. doi: 10.1093/bib/bbv090
- Chen, G., Yang, D., Yang, Y., Li, J., Cheng, K., Tang, G., et al. (2015). Amino acid metabolic dysfunction revealed in the prefrontal cortex of a rat model of depression. *Behav. Brain Res.* 278, 286–292. doi: 10.1016/j.bbr.2014.05.027
- Christoffel, D. J., Golden, S. A., and Russo, S. J. (2011). Structural and synaptic plasticity in stress-related disorders. *Rev. Neurosci.* 22, 535–549. doi: 10.1515/ms.2011.044
- Denmark, A., Tien, D., Wong, K., Chung, A., Cachat, J., Goodspeed, J., et al. (2010). The effects of chronic social defeat stress on mouse self-grooming behavior and its patterning. *Behav. Brain Res.* 208, 553–559. doi: 10.1016/j.bbr.2009.12.041
- Du, H., Wang, K., Su, L., Zhao, H., Gao, S., Lin, Q., et al. (2016). Metabonomic identification of the effects of the Zhimu-Baihe saponins on a chronic



# A Comparative Study of the Diagnostic Potential of Plasma and Erythrocytic $\alpha$ -Synuclein in Parkinson's Disease

Luxuan Wang<sup>a,b</sup> Guowei Wang<sup>a,b</sup> Yangyang Duan<sup>a,b</sup> Feng Wang<sup>c</sup>  
Shaoqing Lin<sup>d</sup> Fengting Zhang<sup>a,b</sup> Hui Li<sup>e</sup> Andy Li<sup>f</sup> Haining Li<sup>b</sup>

<sup>a</sup>School of Clinical Medicine, Ningxia Medical University, Yinchuan, China; <sup>b</sup>Department of Neurology, General Hospital of Ningxia Medical University, Ningxia Key Laboratory of Cerebrocranial Diseases, Incubation Base of National Key Laboratory, Yinchuan, China; <sup>c</sup>Department of Neurosurgery, General Hospital of Ningxia Medical University, Ningxia Key Laboratory of Cerebrocranial Diseases, Incubation Base of National Key Laboratory, Yinchuan, China; <sup>d</sup>Department of Neurology, Brain Center of Sunshine Union Hospital, Sunshine Union Hospital, Weifang, China; <sup>e</sup>Department of Computer Science, Jiangsu Ocean University, Lianyungang, China; <sup>f</sup>Department of Pharmaceutical Sciences, Biomanufacturing Research Institute Biotechnology Enterprise (BRITE), North Carolina Central University, Durham, NC, USA

## Keywords

Parkinson's disease · Peripheral biomarker ·  $\alpha$ -Synuclein · Plasma · Erythrocyte

## Abstract

**Background:** Parkinson's disease (PD) is a neurodegenerative disease characterized by intracellular  $\alpha$ -synuclein ( $\alpha$ -Syn) deposition. Alteration of the  $\alpha$ -Syn expression level in plasma or erythrocytes may be used as a potential PD biomarker. However, no studies have compared their prognostic value directly with the same cohort. **Methods:** The levels of  $\alpha$ -Syn in plasma and erythrocytes, obtained from 45 PD patients and 45 control subjects, were measured with enzyme-linked immunosorbent assay. Then, correlation and receiver operating characteristic curve (ROC) analysis were performed to characterize the predictive power of erythrocytic and plasma

$\alpha$ -Syn. **Results:** Our results showed that  $\alpha$ -Syn expression levels in both plasma and erythrocytes were significantly higher in PD patients than in control subjects ( $823.14 \pm 257.79$  vs.  $297.10 \pm 192.82$  pg/mL,  $p < 0.0001$  in plasma;  $3,104.14 \pm 143.03$  vs.  $2,944.82 \pm 200.41$  pg/mL,  $p < 0.001$  in erythrocytes, respectively). The results of the ROC analysis suggested that plasma  $\alpha$ -Syn exhibited better predictive power than erythrocytic  $\alpha$ -Syn with a sensitivity of 80.0%, specificity of 97.7%, and a positive predictive value of 77.8%. The expression level of plasma  $\alpha$ -Syn correlated well with the age of patients, H-Y stage, MoCA scale, and UPDRS motor scale. On the contrary, there was no correlation between erythrocytic  $\alpha$ -Syn level and clinical parameters in this study. **Conclusion:** Our results suggest that plasma  $\alpha$ -Syn could be a specific and sensitive potential diagnostic biomarker for PD.

© 2020 S. Karger AG, Basel

L.W. and G.W. contributed equally to this article.

Haining Li  
Department of Neurology  
General Hospital of Ningxia Medical University  
No. 804, Shengli Street, Xingqing District, Yinchuan 750000 (China)  
lhnrwww@126.com

Andy Li  
Department of Pharmaceutical Sciences  
Biomanufacturing Research Institute Biotechnology Enterprise (BRITE)  
North Carolina Central University, 1801 Fayetteville Street, Durham, NC 27707 (USA)  
pli@ncsu.edu

KARGER

© 2020 S. Karger AG, Basel

karger@karger.com  
www.karger.com/tdd

## Introduction

Parkinson's disease (PD) is the second most common neurodegenerative disease. Approximately 15 per 100,000 people suffer from this disorder every year [1]. As a progressive neurological disorder, it begins years before the point of diagnosis. Currently, there is no definitive diagnostic approach to detect PD at an early stage. In a clinical setting, the diagnosis of PD is based on motor symptoms or response to dopaminergic drugs [2, 3]. The heterogeneity of clinical features has prompted attempts to find a reliable early diagnostic biomarker, which is crucial for physicians to optimize the early intervention and monitor disease progression and patient responses to treatment.

A body of literature has documented that  $\alpha$ -synuclein ( $\alpha$ -Syn) protein in particular is implicated in the pathologic abnormalities associated with PD, as it is a major component of Lewy bodies [4–6]. Given its critical role in PD pathogenesis,  $\alpha$ -Syn might be a promising candidate as a biomarker for diagnosing PD. Until now, dysregulated  $\alpha$ -Syn has been identified in cerebrospinal fluid, blood, and saliva [7–9]. Thus, determining the best source for  $\alpha$ -Syn detection is a pressing need. As peripheral blood is easily accessible and requires a comparatively less invasive procedure, it would be the preferable source for  $\alpha$ -Syn detection, particularly for screening in populations at early disease stages [10]. Intensive efforts to study alternation of  $\alpha$ -Syn in two major components of blood, plasma, and erythrocyte are underway. Wang et al. [11] have reported that  $\alpha$ -Syn oligomer levels were higher in PD subjects than that in healthy controls, and the ratio of  $\alpha$ -Syn oligomer/total protein ratio exhibited good diagnostic power, with a sensitivity of 79.0% and specificity of 64.7%. Moreover, research by Lin et al. [12, 13] demonstrated that plasma levels of  $\alpha$ -Syn are associated with motor dysfunction and cognitive decline in patients with PD. Until now, most previous studies have focused separately on the relationship between PD and the levels of  $\alpha$ -Syn from plasma or erythrocytes. There has been no comparative study that investigated the prognostic power of plasma and erythrocyte  $\alpha$ -Syn obtained from the same cohort of patients.

In the present study, we quantified total  $\alpha$ -Syn amounts in the plasma and erythrocytes of people with PD and of normal people by a sandwich enzyme-linked immunosorbent assay (ELISA) to explore the underlying correlation between the pathogenesis of PD and the levels of  $\alpha$ -Syn in plasma and erythrocytes, and to compare their predicting potential in the diagnosis of PD.

**Table 1.** Clinical data and red blood cell parameters of the study population

	Healthy controls	PD patients
Cases	45	45
Gender (female/male)	15/30	18/27
Age, years	58.3±16.5	61.8±9.6
Disease duration, years	–	5.07±3.15
UPDRS score	–	25.31±15.94
MoCA scale	–	20.00±6.64
H-Y stage	–	1.98±0.75
NMSS scale	–	54.82±31.92
HAM-D scale	–	8.51±7.44

Data are presented as *n* or the mean ± SD.

## Materials and Methods

### Participants and Groups

Forty-five patients with PD were recruited from the Departments of Neurology of the General Hospital of Ningxia Medical University according to the UK Parkinson's Disease Brain Bank criteria [14]. The exclusion criteria were other neurological diseases, dementia, history of family PD, and other signs of blood disease. In parallel, another 45 age- and sex-matched healthy volunteers with no history of neurological diseases were recruited to the control group (Table 1). All protocols in this study were approved by the Institutional Review Board for human studies at Ningxia Medical University, Ningxia, China (2019-160). Patient consent forms were obtained from all participants.

### Clinical Assessment

Standard clinical scores were used to assess Parkinson's patients: non-motor symptoms were measured using the Non-Motor Symptoms Scale (NMSS) and Montreal Cognitive Assessment (MoCA). Patients' levels of depression were assessed with the Hamilton Depression Rating Scale (HAM-D) and motor symptoms with the Unified Parkinson Disease Rating Scale (UPDRS) part 2 and 3. The stage of PD was determined with the Hoehn and Yahr (H-Y) staging scale. Evaluations were conducted while patients were on standard antiparkinsonian medications.

### Blood Sample Collection

Blood samples (10 mL) were obtained with a 20-G needle (BD, Franklin Lakes, NJ, USA) from the median vein of subjects. All samples and buffers were kept at a temperature of  $-4^{\circ}\text{C}$ . Plasma and erythrocytes were separated by centrifugation for 20 min at 2,200 g. Then the plasma and erythrocytes were stored at a temperature of  $-80^{\circ}\text{C}$  until analysis. Blood sample collections were conducted on the same day as the clinical assessment.

### Measurement of $\alpha$ -Syn Concentration with ELISA

The ELISA analysis of  $\alpha$ -Syn concentration was carried out as described previously [11]. The colorimetric reaction was initiated by the addition of yellow para-nitrophenylphosphatase (pNPP; Sigma) to each well, and absorbance values at 405 and 603 nm were measured on a EL312e microplate reader (Bio-Tek, Winooski, VT, USA).

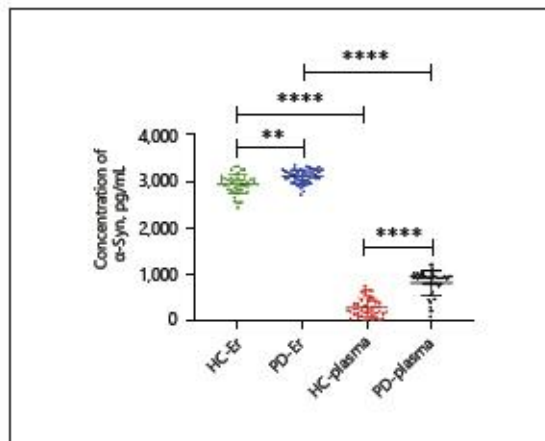


**Fig. 1.** Total level of  $\alpha$ -Syn in plasma/erythrocytes (Er) from PD patients and healthy controls (HC) by ELISA. Data are presented as the mean  $\pm$  SD. \*\*  $p < 0.01$ , \*\*\*\*  $p < 0.0001$ ,  $n = 45$  per group.

#### Statistical Analysis

All data were statistically analyzed by GraphPad Prism 7.0 (GraphPad Software Inc., San Diego, CA, USA) using one-way ANOVA. Pearson's correlation was used to correlate the concentration of plasma or erythrocytic  $\alpha$ -Syn with the clinical parameters. The area under the receiver operating characteristic curve (ROC) was performed for predictive power estimation. The investigator who performed the statistical analysis was blind to the experimental groups. All experiments were performed with 45 replicates. The data are presented as the mean  $\pm$  SD. Differences were considered significant for two-sided  $p$  values  $< 0.05$ .

## Results

### Demographic Characteristics of the Patients

The average age of the PD patients was  $61.8 \pm 9.6$  years (range 31–80), including 27 males and 18 females; the average age of the healthy control patients was  $58.3 \pm 16.5$  years (range 35–84), including 30 males and 15 females. There was no significant difference in the age and gender ratio between the two groups. The disease parameters of the PD patients were assessed, including age, UPDRS, MoCA, H-Y stage, HAM-D scale, and NMMS scale, and are presented in Table 1.

### ELISA Assay of $\alpha$ -Syn

ELISA analysis was performed to evaluate  $\alpha$ -Syn levels in plasma and erythrocytes. As shown in Figure 1,  $\alpha$ -Syn was detected in both plasma and erythrocytes of all groups. The

levels of  $\alpha$ -Syn from plasma and erythrocytes were significantly increased in PD patients compared with the healthy controls ( $p = 0.0017$ ;  $n = 45$ ;  $p < 0.0001$ ;  $n = 45$ , respectively). The expression level of  $\alpha$ -Syn in erythrocytes was significantly higher than that in plasma ( $p < 0.0001$ ;  $n = 45$ ).

### ROC Curves and Correlation Analysis

To determine whether  $\alpha$ -Syn from plasma or erythrocytes could serve as a biomarker for the diagnosis of PD, correlations between clinical parameters and the levels of  $\alpha$ -Syn were analyzed. Our results failed to show a correlation between erythrocytic  $\alpha$ -Syn and the disease parameters, including age of patients, UPDRS motor score, H-Y stage, NMSS, MoCA, and HAM-D scale. However, we found that the expression level of  $\alpha$ -Syn detected in plasma correlated well with the H-Y stage ( $p = 0.023$ ,  $r = 0.341$ ; Fig. 2b), age of patients ( $p < 0.0001$ ,  $r = -0.910$ ; Fig. 3a), UPDRS motor score ( $p = 0.0002$ ,  $r = 0.532$ ; Fig. 4d), and MoCA scale ( $p = 0.0023$ ,  $r = 0.468$ ; Fig. 4a).

We further evaluated the sensitivity and specificity of  $\alpha$ -Syn obtained from plasma or erythrocytes in screening PD with ROC analysis (Fig. 5). Our results showed that plasma  $\alpha$ -Syn had a better predictive performance than erythrocytic  $\alpha$ -Syn. The sensitivity and specificity of plasma  $\alpha$ -Syn were 80.0 and 97.7%, and those of erythrocytic  $\alpha$ -Syn were 69.6 and 76.1%. The positive predictive value of plasma and erythrocytic  $\alpha$ -Syn were 77.8 and 45.7%, respectively (Table 2).

## Discussion

Neurochemical biomarkers, such as  $\alpha$ -Syn, have long held promise in the field of PD for improving diagnosis and are helpful in monitoring disease progression [15, 16]. Among the different sources of tissue sampling, peripheral blood has raised interest in scientists, because it is abundant, easily accessible, and a well-tolerated procedure for patients. Despite the postulated roles of  $\alpha$ -Syn in blood compartments (plasma and erythrocytes) as potential candidates for the prognostic assessment of PD, determining the better biomarker is a pressing need. In the present study, we quantified the level of both erythrocytic  $\alpha$ -Syn and plasmic  $\alpha$ -Syn obtained from the same group of patients and compared their prognostic value.

The literature reports regarding  $\alpha$ -Syn in plasma and erythrocytes in PD patients remain controversial, ranging from an increase to a decrease or unaffected when compared with healthy controls [17–19]. In this study, we found that the  $\alpha$ -Syn in erythrocytes was significantly higher than

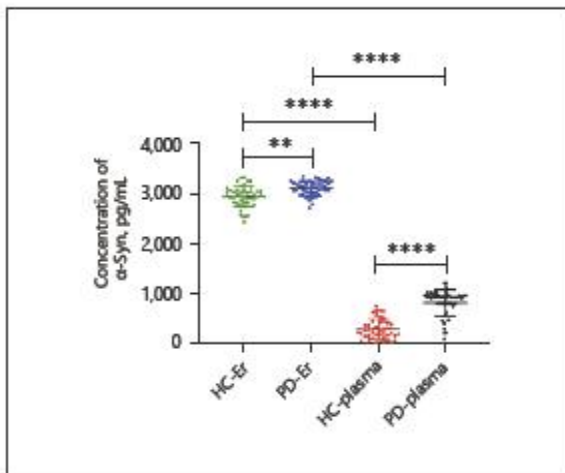


**Fig. 1.** Total level of  $\alpha$ -Syn in plasma/erythrocytes (Er) from PD patients and healthy controls (HC) by ELISA. Data are presented as the mean  $\pm$  SD. \*\*  $p < 0.01$ , \*\*\*\*  $p < 0.0001$ ,  $n = 45$  per group.

#### Statistical Analysis

All data were statistically analyzed by GraphPad Prism 7.0 (GraphPad Software Inc., San Diego, CA, USA) using one-way ANOVA. Pearson's correlation was used to correlate the concentration of plasma or erythrocytic  $\alpha$ -Syn with the clinical parameters. The area under the receiver operating characteristic curve (ROC) was performed for predictive power estimation. The investigator who performed the statistical analysis was blind to the experimental groups. All experiments were performed with 45 replicates. The data are presented as the mean  $\pm$  SD. Differences were considered significant for two-sided  $p$  values  $< 0.05$ .

## Results

#### Demographic Characteristics of the Patients

The average age of the PD patients was  $61.8 \pm 9.6$  years (range 31–80), including 27 males and 18 females; the average age of the healthy control patients was  $58.3 \pm 16.5$  years (range 35–84), including 30 males and 15 females. There was no significant difference in the age and gender ratio between the two groups. The disease parameters of the PD patients were assessed, including age, UPDRS, MoCA, H-Y stage, HAM-D scale, and NMMS scale, and are presented in Table 1.

#### ELISA Assay of $\alpha$ -Syn

ELISA analysis was performed to evaluate  $\alpha$ -Syn levels in plasma and erythrocytes. As shown in Figure 1,  $\alpha$ -Syn was detected in both plasma and erythrocytes of all groups. The

levels of  $\alpha$ -Syn from plasma and erythrocytes were significantly increased in PD patients compared with the healthy controls ( $p = 0.0017$ ;  $n = 45$ ;  $p < 0.0001$ ;  $n = 45$ , respectively). The expression level of  $\alpha$ -Syn in erythrocytes was significantly higher than that in plasma ( $p < 0.0001$ ;  $n = 45$ ).

#### ROC Curves and Correlation Analysis

To determine whether  $\alpha$ -Syn from plasma or erythrocytes could serve as a biomarker for the diagnosis of PD, correlations between clinical parameters and the levels of  $\alpha$ -Syn were analyzed. Our results failed to show a correlation between erythrocytic  $\alpha$ -Syn and the disease parameters, including age of patients, UPDRS motor score, H-Y stage, NMSS, MoCA, and HAM-D scale. However, we found that the expression level of  $\alpha$ -Syn detected in plasma correlated well with the H-Y stage ( $p = 0.023$ ,  $r = 0.341$ ; Fig. 2b), age of patients ( $p < 0.0001$ ,  $r = -0.910$ ; Fig. 3a), UPDRS motor score ( $p = 0.0002$ ,  $r = 0.532$ ; Fig. 4d), and MoCA scale ( $p = 0.0023$ ,  $r = 0.468$ ; Fig. 4a).

We further evaluated the sensitivity and specificity of  $\alpha$ -Syn obtained from plasma or erythrocytes in screening PD with ROC analysis (Fig. 5). Our results showed that plasma  $\alpha$ -Syn had a better predictive performance than erythrocytic  $\alpha$ -Syn. The sensitivity and specificity of plasma  $\alpha$ -Syn were 80.0 and 97.7%, and those of erythrocytic  $\alpha$ -Syn were 69.6 and 76.1%. The positive predictive value of plasma and erythrocytic  $\alpha$ -Syn were 77.8 and 45.7%, respectively (Table 2).

## Discussion

Neurochemical biomarkers, such as  $\alpha$ -Syn, have long held promise in the field of PD for improving diagnosis and are helpful in monitoring disease progression [15, 16]. Among the different sources of tissue sampling, peripheral blood has raised interest in scientists, because it is abundant, easily accessible, and a well-tolerated procedure for patients. Despite the postulated roles of  $\alpha$ -Syn in blood compartments (plasma and erythrocytes) as potential candidates for the prognostic assessment of PD, determining the better biomarker is a pressing need. In the present study, we quantified the level of both erythrocytic  $\alpha$ -Syn and plasmic  $\alpha$ -Syn obtained from the same group of patients and compared their prognostic value.

The literature reports regarding  $\alpha$ -Syn in plasma and erythrocytes in PD patients remain controversial, ranging from an increase to a decrease or unaffected when compared with healthy controls [17–19]. In this study, we found that the  $\alpha$ -Syn in erythrocytes was significantly higher than

**Fig. 2.** Correlation analysis of H-Y stage with plasma (a, b) and erythrocytic (c, d)  $\alpha$ -Syn expression levels in PD patients. a, c Mean  $\alpha$ -Syn levels among H-Y stages of PD patients tested. b, d Correlation analysis of H-Y stages of PD patients and  $\alpha$ -Syn expression levels. H-Y stage; \*  $p < 0.05$ ,  $n = 6-12$  per group.

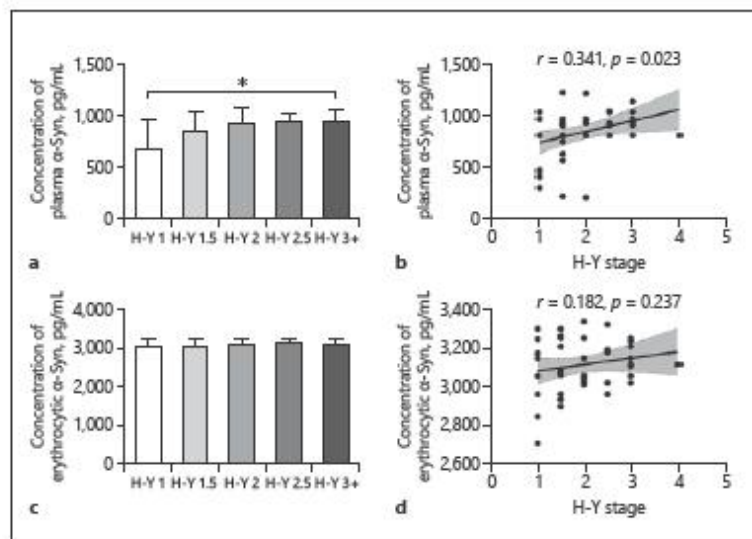
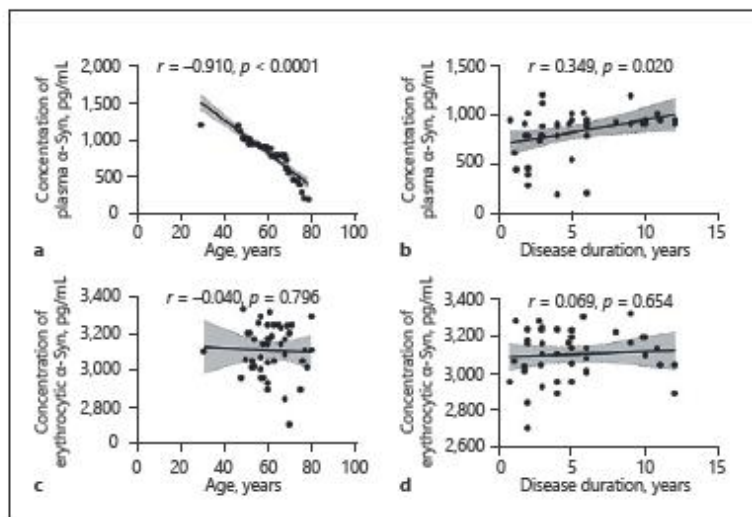


**Fig. 3.** Correlation analysis of age (a, c) and disease duration (b, d) with plasma (a, b) and erythrocytic (c, d)  $\alpha$ -Syn expression levels in PD patients.  $n = 45$  per group.



that in plasma, which was consistent with previous findings showing that most of the  $\alpha$ -Syn in human blood resides in the erythrocytes [20]. Additionally, the level of total  $\alpha$ -Syn detected from both erythrocytes and plasma in PD patients was remarkably increased compared to that of control subjects. These results were in accordance with previous studies [17, 18]. These inconsistent results may be caused by

hemolysis contamination during sampling, different analysis methods, and the diversity of disease severity. Furthermore, correlation analysis between the level of  $\alpha$ -Syn and the clinical parameters was conducted to determine their role in the diagnosis of PD. The results of ROC analysis indicated that plasmic  $\alpha$ -Syn has a better predictive performance than erythrocytic  $\alpha$ -Syn.

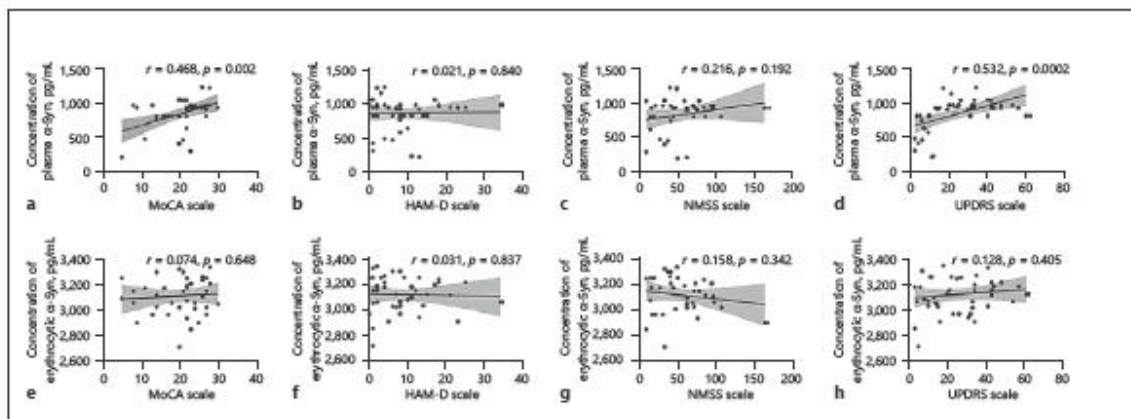


**Fig. 4.** Correlation analysis of motor and non-motor symptoms with plasma (a–d) and erythrocytic (e–h)  $\alpha$ -Syn expression levels in PD patients: MoCA scale (a, e), HAM-D scale (b, f), NMSS scale (c, g), and UPDRS scale (d, h).  $n = 45$  per group.

Neurodegenerative diseases, such as PD, have always been linked to aging [21, 22] and the aberrant  $\alpha$ -Syn accumulation contributes to the pathogenesis of PD, which would worsen motor deficits and disease severity [23, 24]. We found that the levels of  $\alpha$ -Syn in erythrocytes and plasma increased with the disease duration, and a significant correlation was found between disease duration and the expression level of plasma  $\alpha$ -Syn. However, the amount of  $\alpha$ -Syn in plasma inversely correlated well with the age of PD patients, and an inverse correlation between the level of erythrocytic  $\alpha$ -Syn and age was also found, albeit without statistical significance. Our results support previous research and demonstrates that the level of  $\alpha$ -Syn could be overcome by the effect of age [25].

PD is a progressive, neurodegenerative disorder that is characterized by severe motor symptoms, including uncontrollable tremor, postural imbalance, slowness of movement, and rigidity. Non-motor symptoms are extremely frequent and important components of PD. In two recent studies, at least one non-motor symptom was reported by almost 100% of patients [26, 27]. Non-motor symptoms of PD could manifest many years before motor symptoms and be predominant as the disease advances [28]. Previous literature has documented that  $\alpha$ -Syn deposition was related to motor deficits and non-motor features in PD [29, 30]. In order to investigate the relationship between the level of  $\alpha$ -Syn and symptoms and stage of PD, correlation analyses were performed. Our results showed that there was no correlation between the expression level of erythrocytic  $\alpha$ -Syn and clinical features of PD

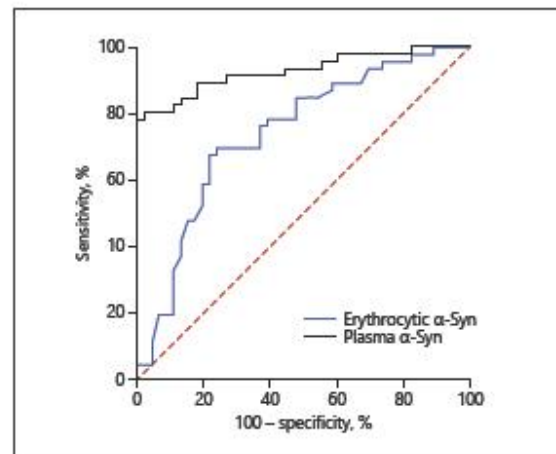


**Fig. 5.** ROC analysis of the total level of  $\alpha$ -Syn in plasma/erythrocytes as a PD biomarker.

patients; however, there were strong positive correlations between plasma  $\alpha$ -Syn levels and MoCA, plasma  $\alpha$ -Syn levels and H-Y stage, and plasma  $\alpha$ -Syn levels and the UPDRS scale in this study. Herein, our results showed that the level of plasma  $\alpha$ -Syn could serve as a biomarker for the severity and progression of PD. However, Malec-Litwinowicz et al. [31] reported that the level of plasma  $\alpha$ -Syn has an inverse correlation with the severity of motor symptoms. We proposed that this discrepancy might be

**Table 2.** Comparison of the predictive power of plasma and erythrocytic  $\alpha$ -Syn for PD

	Sensitivity, %	Specificity, %	Accuracy, %	Area under ROC curve (95% CI)
Erythrocytic $\alpha$ -Syn	69.6	76.1	45.7	0.741 (0.6380–0.8437)
Plasma $\alpha$ -Syn	80.0	97.7	77.8	0.926 (0.8699–0.9829)

caused by a difference in motor subtypes and severity of PD [32, 33], as well as the small sample size of this study.

Erythrocytes are emerging as a valid peripheral model for the study of aging-related pathologies [34, 35]. Evidence indicates that erythrocytes lose all of their organelles when they mature, resulting in a lack of potential to replace proteins that have lost their functions and making them highly sensitive to any aberrations [36–38]. However, based on our observation, we found that plasma-derived  $\alpha$ -Syn has better predictive power than that in erythrocytes. We hypothesized that this might be caused by the form of  $\alpha$ -Syn we used. In the present study, we analyzed the level of total  $\alpha$ -Syn in both plasma and erythrocytes. There were three forms of  $\alpha$ -Syn, including oligomeric/aggregated, and phosphorylated  $\alpha$ -syn.  $\alpha$ -Syn oligomers in erythrocytes [39] and oligomeric [40, 41] and phosphorylated [42]  $\alpha$ -Syn in plasma have been reported to be associated with its mechanisms of toxicity. For example, phosphorylated at Ser129 (pS129)  $\alpha$ -Syn was able to discriminate patients with PD from neurologically normal controls, with a sensitivity and a specificity of 72 and 68%, respectively [43]. Moreover, Miranda et al. [44] reported that posttranslational modifications in  $\alpha$ -Syn are linked to the pathobiology of PD, and a combinatory analysis of the levels of Y125 phosphorylated, Y39 nitrated, and glycosylated  $\alpha$ -Syn in erythrocytes resulted in an increased sensitivity.

Some limitations should be noted in this study. First are the relatively small number of enrolled subjects for correlation analysis and the cross-sectional design. Second, other forms of  $\alpha$ -Syn, such as oligomeric and phosphorylated forms, were not measured in our study. In the future, a longitudinal study with large cohorts is needed to validate our results.

## Conclusion

This study provides evidence that plasma  $\alpha$ -Syn has a better prognostic performance than erythrocytic  $\alpha$ -Syn. Furthermore, the plasma  $\alpha$ -Syn level, which correlated with motor symptom severity, could serve as a non-invasive biomarker for predicting motor decline in PD.

## Acknowledgements

The authors greatly appreciate Ms. Roslyn Lewis for language checking and proof reading.

## Statement of Ethics

This study was conducted ethically in accordance with the World Medical Association Declaration of Helsinki. The study was approved by the local ethical committee and all participants gave written informed consent.

## Disclosure Statement

The authors declare that they have no competing interests.

## Funding Sources

This work is supported by a grant from the National Science Foundation of China (81460179) to Ha.L., and the Key Research and Development Program of Ningxia (2018BFG02007 and 2019BEB04008).

## Author Contributions

The work presented here was carried out in collaboration with all authors. Ha.L., and A.L. designed the study and reviewed and edited the manuscript. L.W. performed the experiments, collected the data, performed the statistical analysis and drafted the manuscript. G.W., S.L., F.W. performed the experiments and data collection. Y.D., F.Z., and Hu.L. performed the data analysis and interpretation. All authors read and approved the final manuscript.

## References

- 1 Tysnes OB, Storstein A. Epidemiology of Parkinson's disease. *J Neural Transm (Vienna)*. 2017 Aug;124(8):901–5.
- 2 Kalia LV, Lang AE. Parkinson's disease. *Lancet*. 2015 Aug;386(9996):896–912.
- 3 Chaudhuri KR, Schapira AH. Non-motor symptoms of Parkinson's disease: dopaminergic pathophysiology and treatment. *Lancet Neurol*. 2009 May;8(5):464–74.

## Knockdown of Mg<sup>2+</sup>/Mn<sup>2+</sup> dependent protein phosphatase 1A promotes apoptosis in BV2 cells infected with *Brucella suis* strain 2 vaccine

JUAN YANG<sup>1\*</sup>, GUOWEI WANG<sup>1\*</sup>, HAINING LI<sup>1\*</sup>, WENLI ZHENG<sup>1</sup>, BURUI GUO<sup>1</sup> and ZHENHAI WANG<sup>1,2</sup>

<sup>1</sup>Department of Neurology, The General Hospital of Ningxia Medical University;

<sup>2</sup>Ningxia Key Laboratory of Cerebrocranial Diseases, Incubation Base of National Key Laboratory, Yinchuan, Ningxia 750004, P.R. China

Received January 16, 2019; Accepted December 10, 2019

DOI: 10.3892/etm.2020.8745

**Abstract.** The ability to inhibit host macrophage apoptosis is one of the survival strategies of intracellular bacteria, including *Brucella*. In the present study the role of Mg<sup>2+</sup>/Mn<sup>2+</sup> dependent protein phosphatase 1A (PPM1A) in the apoptosis of *Brucella suis* (*B. suis*) strain 2 vaccine-infected BV2 cells was investigated. Compared with control cells, the protein expression levels of cleaved caspase-3 were markedly increased in PPM1A short hairpin (sh)RNA-transfected BV2 cells. Flow cytometry analysis showed that treatment with JNK activator anisomycin significantly increased the rate of apoptosis in BV2 cells in comparison with the control cells. Furthermore, PPM1A shRNA significantly increased the levels of JNK phosphorylation and the levels of cleaved caspase-3 in BV2 cells infected with *B. suis* strain 2 in comparison with the control cells. DAPI staining showed nuclear condensation in *B. suis* infected BV2 cells transfected with PPM1A shRNA in comparison with the control shRNA cells. Flow cytometry analysis showed that PPM1A shRNA significantly increased the percentage of apoptotic BV2 cells infected with *B. suis* strain 2 compared with those transfected with control shRNA. Taken together, these data suggested that knockdown of PPM1A promotes apoptosis in *B. suis* strain 2-infected BV2 cells and that PPM1A may be a potential target in the development of treatments to inhibit intracellular growth of *B. suis*.

### Introduction

Brucellosis is a zoonotic infectious disease caused by infection with the bacterial genus *Brucella*. *Brucella* are able to localize to phagocytic cells in human organs including the liver, spleen, bone marrow and brain, thereby leading to various clinical manifestations (1). *Brucella suis* (*B. suis*) can cause devastating multi-organ diseases in humans, which lead to severe health complications (2-4). Previous studies have shown that *Brucella* has several strategies to establish chronic infection, including inhibition of apoptosis in infected mononuclear cells, inhibition of dendritic cell maturation, and a reduction in the antigen presentation ability and activation of naïve T-cells (5,6). One possible strategy for treatment of *B. suis* infection is the promotion of apoptosis in host cells. *B. suis* strain 2 is a low virulence live-strain vaccine known to improve cellular immunity and protect animals against infection by heterologous virulent *Brucella* (7). The properties of *B. suis* strain 2 make it a suitable model for *in vitro* study of *Brucella*.

Mg<sup>2+</sup>/Mn<sup>2+</sup> dependent protein phosphatase 1A (PPM1A), a member of the serine/threonine phosphatase family, is known to be a critical regulator of cellular apoptosis (8). It has been shown that PPM1A is a key factor in the innate antibacterial and antiviral response of macrophages, particularly in *Mycobacterium tuberculosis* infection (9,10). As both *Brucella* and *Mycobacterium tuberculosis* effectively function as intracellular parasites, sharing similarities in their pathogenesis (11,12) it is hypothesized in the present study that PPM1A may also regulate apoptosis in *B. suis* infection.

Microglia, resident immune cells in the brain, are involved in normal brain development and neuronal recovery (13). It has been reported that *Brucella* infection activates microglia and leads to neuronal loss, thereby contributing to neurological deficits observed during neurobrucellosis. In the present study, the role of PPM1A in the regulation of apoptosis was investigated in BV2 cells, an immortalized mouse cell line that models microglia, that had been infected with *B. suis* strain 2.

**Correspondence to:** Dr Zhenhai Wang, Department of Neurology, The General Hospital of Ningxia Medical University, 804 South Shengli Street, Yinchuan, Ningxia 750004, P.R. China  
E-mail: wangzhenhai1968@163.com

\*Contributed equally

**Key words:** Mg<sup>2+</sup>/Mn<sup>2+</sup> dependent protein phosphatase 1A, JNK, apoptosis, *Brucella suis* vaccine strain 2, microglia, BV2 cells



## Materials and methods

**Cell lines and bacteria.** Mouse microglia cell line BV2 cells were provided by American Type Culture Collection and cultured in DMEM (Thermo Fisher Scientific Inc.) containing 10% FBS (Hyclone; GE Healthcare Life Sciences), 2 mM glutamine and 200 mM streptomycin/penicillin (Beijing Solarbio Science and Technology Co., Ltd.) and maintained in 5% CO<sub>2</sub> at 37°C. *B. suis* strain 2 was a kind gift from Professor Xu of Ningxia Medical University (Yinchuan, China) and was cultured on trypticase soy-agar plates at 37°C in a 5% CO<sub>2</sub> incubator. Individual *B. suis* strain 2 colonies were seeded in sterilized trypticase soy broth solution at 37°C in 5% CO<sub>2</sub>. Bacteria were harvested by centrifugation for 20 min at 2,000 g at 4°C and washed twice with PBS. Bacterial density in the culture was estimated using a McFarland standards kit (bioMérieux China Ltd.). All experiments involving bacteria were performed in a biosafety level 2 laboratory.

**In vitro infection.** BV2 cells (8x10<sup>5</sup>) were grown in six-well cell culture plates, allowed to reach 60% confluence, and then exposed to *B. suis* strain 2 at multiplicity of infection (MOI) 100 for 1 h in DMEM without antibiotics. Thereafter, BV2 cells were washed extensively, to remove extracellular bacteria. The infection was maintained for 24 h in the presence of 100 µg/ml gentamicin, to kill any remaining extracellular bacteria. Medium and cells were collected for subsequent experiments. BV2 cells were infected at different intervals (0, 4, 8 and 24 h) for western blotting and at 24 h for the remaining analysis. In addition, BV2 cells were also infected in shRNA experiments.

**Cell viability assay.** Cell viability was determined using a Cell Counting Kit-8 (CCK-8) assay according to the manufacturer's protocol (Nanjing Fengfeng Biomedical Technology Co., Ltd.). In brief, uninfected BV2 cells were seeded in 96-well cell culture plates at a density of 1x10<sup>4</sup> cells/ml and cultured overnight at 37°C. Cells were treated with SP600125 (MedChemExpress; 5 and 10 µM) and anisomycin (MedChem Express; 0.2, 0.5 and 1 µM) for 24 h. Cells treated with DMSO served as controls. Subsequently, CCK-8 solution was added to each well and incubated for an additional 4 h. The absorbance at 450 nm was measured using a microplate reader (BioTek Instruments, Inc.).

**Short hairpin (sh)RNA expression constructs and virus infection.** Lentiviral vector GV493 and an shRNA plasmid coding for PPM1A were purchased from Shanghai Genechem Co., Ltd. The shRNA targeting PPM1A had the sequence 5'-GAGAGT TATGTCAGAGAAGAA-3'. The scrambled RNA sequence, used as a control, had the sequence 5'-TTCTCCGAACGTGTC ACGT-3'. BV2 cells were infected with viruses expressing control shRNA or shRNA targeting PPM1A at MOI 50. BV2 cells were used 72 h after transfection, and stable cell lines were established as previously described and were selected for 5 days using puromycin (Sigma-Aldrich; Merck KGaA; 2 µg/ml) (14).

**Flow cytometry.** BV2 cells (1x10<sup>4</sup> cells) were treated with 5 µM SP600125 or 0.2 µM anisomycin at 37°C for 48 h and stained with annexin V conjugated to FITC or propidium iodide

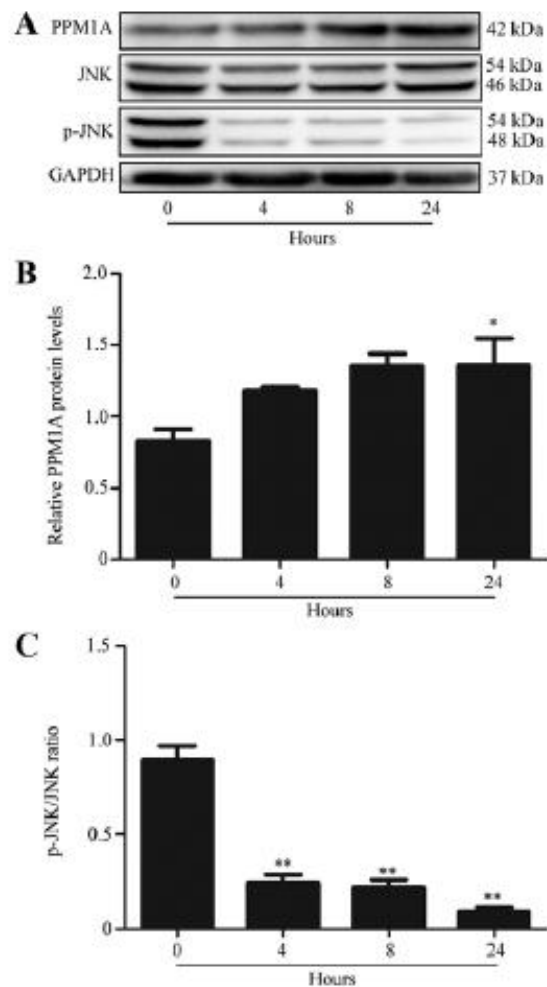


**Figure 1.** Expression of PPM1A and reduced phosphorylation of JNK in *Brucella suis* strain 2-infected BV2 cells. (A) Representative blots from three independent experiments. Quantification of (B) PPM1A and (C) p-JNK protein levels from three separate experiments, normalized to GAPDH. \* $P < 0.05$ , \*\* $P < 0.01$  vs. 0 h. p, phosphorylated; PPM1A, Mg<sup>2+</sup>/Mn<sup>2+</sup> dependent protein phosphatase 1A.

according to the manufacturer's protocol (cat. no. BB-4101-1; Nanjing Fengfeng Biomedical Technology Co., Ltd.). Apoptosis was determined by flow cytometry using a BD Accuri C6. Data analysis was performed using BD Accuri C™ 6 software Plus (BD Biosciences).

**Western blot analysis.** BV2 cells were harvested, washed twice with PBS, and lysed in RIPA buffer (Nanjing Jiancheng Bioengineering Institute). Protein concentrations in the lysates were quantified by the bicinchoninic acid method following the manufacturer's instructions (Nanjing KeyGen Biotech Co., Ltd.). A total of 30 µg of protein per sample was loaded and separated on 12% Mini-Protean® TGX™ gels (Bio-Rad Laboratories, Inc.) and subsequently transferred onto a polyvinylidene difluoride membrane. Prior to antibody incubations, the samples were blocked

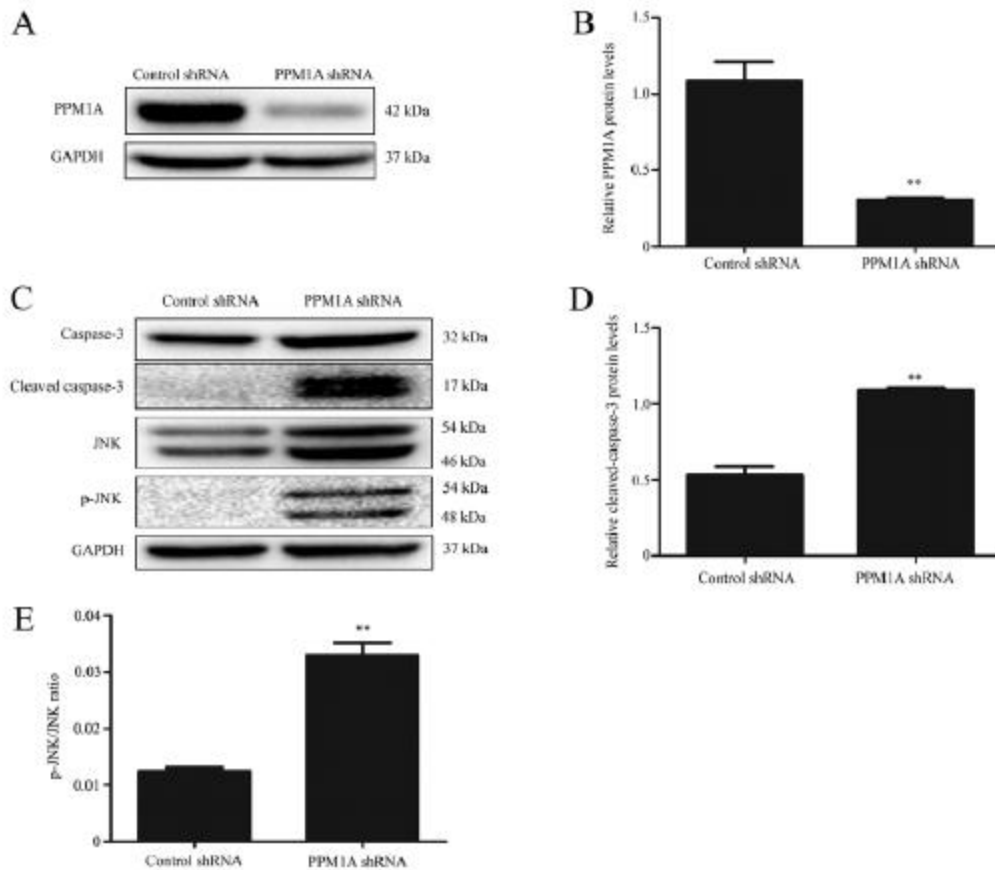


**Figure 2.** Knockdown of PPM1A by transfection of shRNA in BV2 cells. (A) BV2 cells were transfected with PPM1A shRNA and control shRNA, and western blot analysis was performed to determine the protein levels of PPM1A. (B) Densitometry of PPM1A protein levels. (C) Western blot analysis was also performed to assess the levels of caspase-3, cleaved caspase-3, JNK and p-JNK. The blots shown are representative of three independent experiments. Densitometric quantification data is expressed as the intensity ratio of target proteins (D) cleaved caspase-3 and (E) p-JNK to GAPDH. \* $P < 0.01$  vs. control shRNA cells. PPM1A,  $Mg^{2+}/Mn^{2+}$  dependent protein phosphatase 1A; p, phosphorylated; shRNA, short hairpin RNA.

with 5% skimmed milk at room temperature for 1 h. PPM1A (dilution 1:1,000; cat. no. ab14824), JNK (dilution 1:1,000; cat. no. ab179461), phosphorylated (p)-JNK (dilution 1:3,000; cat. no. ab4821), caspase-3 (dilution 1:1,000; cat. no. ab13847), cleaved caspase-3 (dilution 1:500; cat. no. ab2302) and GAPDH (dilution 1:1,000; cat. no. ab181602) protein levels were assessed using specific antibodies (Abcam) at 4°C overnight. Horseradish peroxidase-conjugated goat anti-mouse polyclonal antibody (dilution 1:5,000; Santa Cruz Biotechnology, Inc.; cat. no. sc-2031) was used as the secondary antibody for 30 min at room temperature. The blot was developed using Western Lightning Ultra chemiluminescent substrate (Bio-Rad Laboratories, Inc.) in an EpiChem3 darkroom (UVP, LLC). Image Lab 3.0 software used to analyze the results (Bio-Rad Laboratories, Inc.).

**DAPI staining.** BV2 cells were seeded on six-well plates at a density of  $5 \times 10^5$  cells/ml and cultured overnight at 37°C. Cells were fixed in 4% paraformaldehyde at room temperature for

1 h. After washing with PBS and air-drying for 3 min at room temperature, cells were stained with DAPI at room temperature for 1 min and images were captured using fluorescence microscopy immediately (x200 magnification, 6 random field were viewed).

**Statistical analysis.** All data are presented as the mean  $\pm$  SD from at least three independent experiments. Graphpad Prism 7.0 (GraphPad Software, Inc.) was used for the analysis. Comparisons between indicated groups were performed using one-way analysis of variance followed by Tukey's post-hoc test.  $P < 0.05$  was considered to indicate a statistically significant difference.

## Results

**Increased expression of PPM1A and reduced phosphorylation of JNK are observed in *B. suis* strain 2-infected BV2 cells.** The expression of PPM1A and JNK proteins was evaluated by western blot analysis in BV2 cells at 4, 8 and 24 h post-*B. suis*

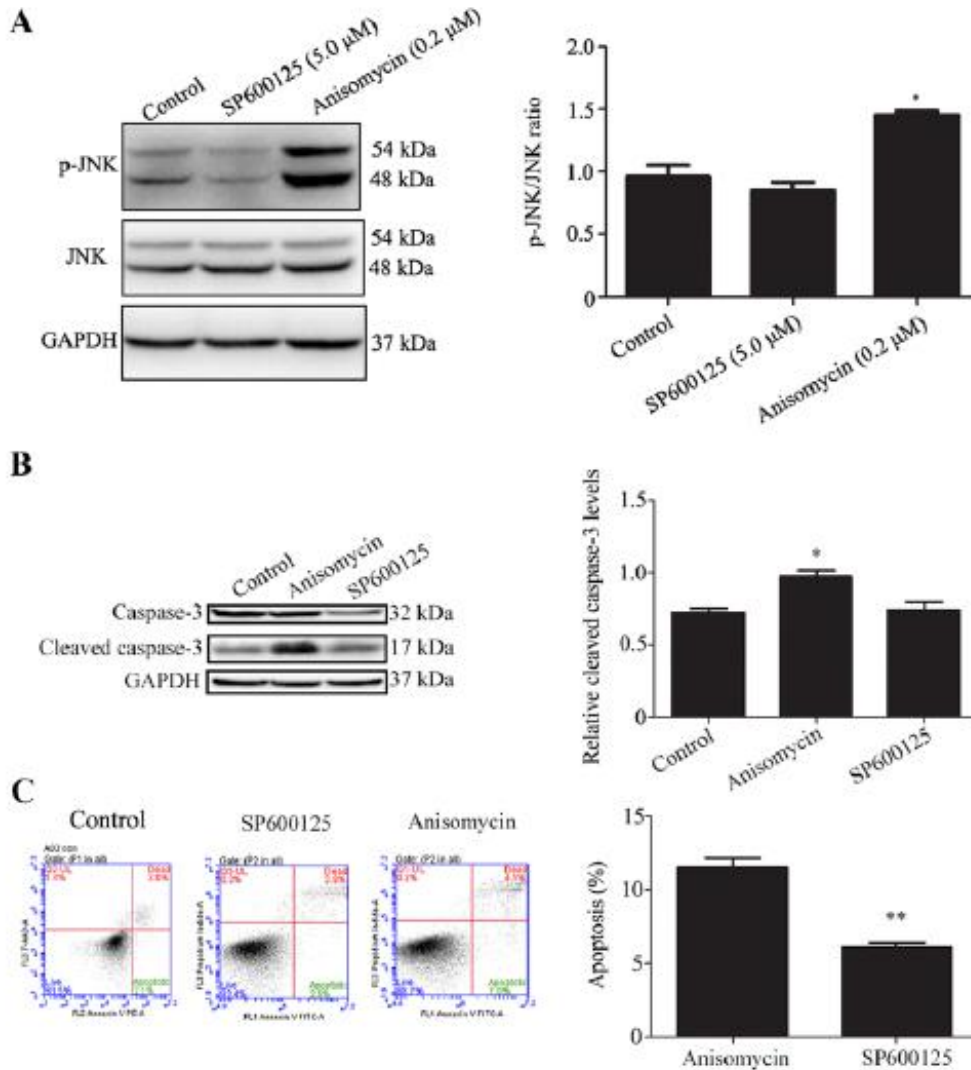


Figure 3. Effects of JNK modulation by SP100625 and anisomycin on apoptosis in BV2 cells. BV2 cells were treated with indicated concentrations of SP100625 or anisomycin, and western blot analysis was used to evaluate the expression of (A) p-JNK and JNK and (B) caspase-3 and cleaved caspase-3. (C) BV2 cells were treated with SP600125 at 5  $\mu$ M or anisomycin at 0.2  $\mu$ M, and stained with Annexin V conjugated to FITC and propidium iodide. The percentage of cells undergoing apoptosis is shown. The total number of apoptotic cells was estimated from the sum of cells in early apoptosis (lower right) and late apoptosis (upper right). \*P<0.05, \*\*P<0.01 vs. control cells. p, phosphorylated.

strain 2 infection. The results indicated that PPM1A expression was significantly increased and phosphorylation of JNK was significantly reduced in a time-dependent manner compared with control shRNA-infected cells (Fig. 1).

*PPM1A knockdown promotes caspase-dependent apoptosis in uninfected BV2 cells.* To further characterize the role of PPM1A in apoptosis regulation, RNA interference was used to knock down PPM1A expression in BV2 cells. The results indicated that PPM1A protein levels in cells transfected with shRNA specific for PPM1A were significantly reduced compared with those transfected with control shRNA (Fig. 2A and B). This suggested that shRNA targeting

PPM1A mRNA could effectively knockdown PPM1A expression at a translational level. Compared with control shRNA cells, the protein expression levels of cleaved caspase-3 were markedly increased in PPM1A shRNA-transfected BV2 cells (Fig. 2C and D). Collectively, these results suggested that knockdown of PPM1A promoted caspase-dependent apoptosis in BV2 cells.

*Activation of JNK signaling promotes apoptosis in BV2 cells.* To determine whether JNK signaling was involved in apoptosis, uninfected BV2 cells were treated with the JNK inhibitor SP100625 or JNK activator anisomycin. The CCK-8 assay showed that treatment with SP600125 at 5  $\mu$ M or aniso-

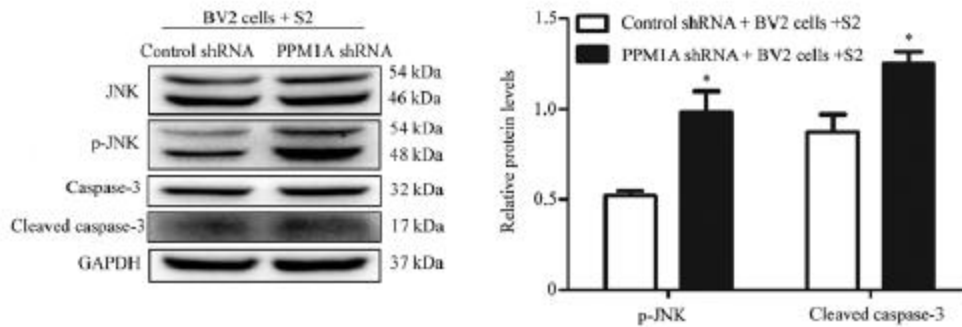


Figure 4. Effects of PPM1A knockdown on protein levels of JNK, p-JNK, caspase-3 and cleaved caspase-3 in BV2 cells infected with *B. suis* s2. BV2 cells infected with *B. suis* s2 were transfected with PPM1A shRNA or control shRNA. Cells were collected for western blot analysis. The blots shown are representative of three independent experiments. Densitometric quantification data are expressed as the intensity ratio of target proteins to total JNK or GAPDH. \* $P < 0.05$  vs. control shRNA + BV2 cells + s2. *B. suis*, *Brucella suis*; PPM1A,  $Mg^{2+}/Mn^{2+}$  dependent protein phosphatase 1A; p, phosphorylated; s2, strain 2; shRNA, short hairpin RNA.

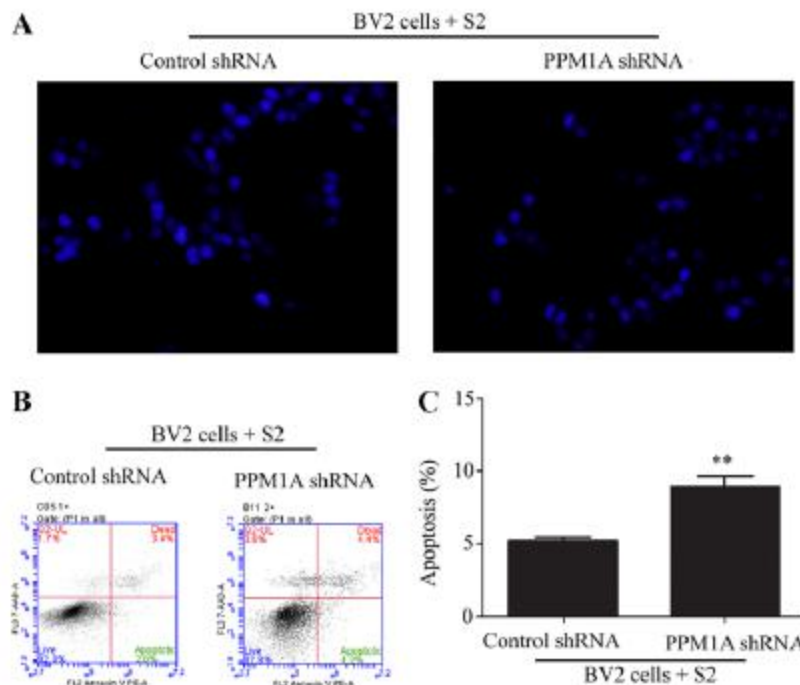


Figure 5. Effects of PPM1A knockdown on apoptosis in BV2 cells infected with *B. suis* s2. BV2 cells infected with *B. suis* s2 were transfected with PPM1A shRNA or control shRNA. (A) Cells were stained with Annexin V conjugated to FITC and PI and harvested for a flow cytometry assay. The total apoptosis levels were estimated as the sum of cells in early apoptosis (lower right) and late apoptosis (upper right). Magnification  $\times 20$ . (B) The number of PI/Annexin V single positive and Annexin V/PI double positive cells was used as a measurement of apoptotic cells (C). Data are expressed as the mean  $\pm$  SD. \*\* $P < 0.01$  vs. control shRNA cells. *B. suis*, *Brucella suis*; s2, strain 2; shRNA, short hairpin RNA; PI, propidium iodide.

mycin at  $0.2 \mu\text{M}$  had no significant effect on BV2 cell viability compared with DMSO-treated cells (data not shown). Western blot analysis showed that SP100625 appeared to reduce and anisomycin markedly increased the levels of JNK phosphorylation in BV2 cells (Fig. 3A). In comparison to vehicle treated cells, the levels of cleaved caspase-3 were significantly increased in BV2 cells treated with anisomycin, but not altered

in those treated with SP100625 (Fig. 3B). To further investigate the effects of JNK signaling modulation on apoptosis in BV2 cells, flow cytometry analysis was performed to detect apoptosis in BV2 cells treated with SP600125 or anisomycin. Treatment with anisomycin significantly increased apoptosis levels in BV2 cells compared with that of the SP600125 treated cells (Fig. 3C).

**Knockdown of PPM1A induces activation of JNK signaling in BV2 cells.** To investigate whether PPM1A regulates JNK phosphorylation, the protein levels of JNK and p-JNK were measured using western blot analysis in BV2 cells transfected with PPM1A shRNA. The results indicated that the level of p-JNK in PPM1A shRNA transfected cells was significantly higher than that in control shRNA transfected cells (Fig. 2E), suggesting that PPM1A knockdown activates JNK signaling in BV2 cells.

**Knockdown of PPM1A promotes apoptosis in BV2 cells infected with *B. suis* strain 2.** The protein levels of JNK, p-JNK, caspase-3 and cleaved caspase-3 were assessed in BV2 cells infected with *B. suis* strain 2 and transfected with PPM1A shRNA. As shown in Fig. 4, PPM1A shRNA significantly increased the ratios of p-JNK/JNK and the expression levels of cleaved caspase-3 in BV2 cells infected with *B. suis* strain 2 compared with control cells. Additionally, flow cytometry analysis showed that PPM1A shRNA significantly increased the level of apoptosis in BV2 cells infected with *B. suis* strain 2 compared with cells treated with control shRNA (Fig. 5A and B). Taken together, these data suggest that knockdown of PPM1A promotes apoptosis in BV2 cells infected with *B. suis* strain 2.

## Discussion

*Brucella* is an intracellular parasite, which previously, the authors of the current study have reported that the outer membrane protein of *Brucella* inhibits host cell apoptosis (15), facilitating the replication of bacteria within the cell. In the present study, knockdown of PPM1A promoted apoptosis in BV2 cells infected with *B. suis* strain 2. Therefore, it is plausible to propose that PPM1A reduces intracellular replication of *B. suis* strain 2 by inducing apoptosis in BV2 cells.

Protein phosphatases are enzymes that catalyze the dephosphorylation of protein molecules in contrast to protein kinases, which phosphorylate proteins. PPM1A is a protein phosphatase, widely present in eukaryotic cells. PPM1A participates in the regulation of the cell cycle, apoptosis, antiviral and other related biological functions (16-18). In the present study, PPM1A was upregulated in BV2 cells infected with *B. suis* strain 2, and knockdown of PPM1A shown to promote apoptosis. PPM1A may be a potential target to promote the apoptosis of *Brucella*-infected cells. In addition, JNK was suggested to be a substrate for PPM1A, and increased phosphorylation of JNK can promote apoptosis. These findings indicate that the PPM1A-JNK pathway may be involved in the regulation of BV2 apoptosis after *B. suis* strain 2 infection. Based on these results, a further study will be focused on the screening of drugs that inhibit PPM1A *in vitro* and observation of whether these drugs can enhance the efficacy of antibacterial therapy.

Brucellosis is more severe in humans than in domestic animals and causes a variety of clinical symptoms (3), including central nervous system infection related symptoms (19,20). The incidence of brucellosis is higher in areas of intensive agriculture and animal husbandry, including Ningxia, China (21,22).

*Brucella* is a common zoonotic pathogen that can survive and proliferate within several types of phagocytic

and non-phagocytic cells. Phagocytic cells are the main host and *Brucella* can inhibit apoptosis of these cells (23). In the absence of effective antibiotics treatment, 50% of brucellosis cases become chronic and cause multiple organ damage, including neurological disorders, bone destruction and cardiovascular damage (24,25). Meningitis is a common cause of fatality in brucellosis (26,27). Improving antibiotic treatment and reducing infection recurrence is the ultimate goal in brucellosis treatment. In the current study, the PPM1A-JNK pathway was revealed to be involved in the regulation of BV2 cell apoptosis after *B. suis* strain 2 infection. Whether PPM1A knockdown can reduce bacterial replication by promoting apoptosis needs to be further explored.

There are several limitations to the present study. Whether only *B. suis* strain 2-infected BV2 cells undergo apoptosis by PPM1A protein expression knockdown has not been elucidated, as it is difficult to distinguish *B. suis* strain 2-infected BV2 cells from uninfected cells. Additionally, the similarity between the *B. suis* strain 2 vaccine used in the present study and wild-type *Brucella* has not been confirmed by sequencing results. This study may inspire the development of new *Brucella* treatments that promote the apoptosis of host cells, so as to reduce the recurrence of infection.

## Acknowledgements

Not applicable.

## Funding

The current study was supported by grants from the National Natural Science Foundation of China (grant no. 31660030) and the First Class Discipline Construction Project in Colleges and Universities of Ningxia (grant no. NXYLKK2017A05).

## Availability of data and materials

The datasets used and/or analyzed during the current study are available from the corresponding author on reasonable request.

## Authors' contributions

JY, GW, HL and ZW conceived and designed the experiments. JY, GW, and HL conducted all the experiments. WZ and BG contributed to the design of parts of the study and collected and analyzed some of the data. All authors read and approved the final manuscript. All authors read and approved the final manuscript.

## Ethics approval and consent to participate

Not applicable.

## Patient consent for publication

Not applicable.

## Competing interests

The authors declare that they have no competing interests.

## References

- Vollmar P, Zange S, Zöller L, Erkel J and Robert Thoma B: Brucellosis, an overview and current aspects. *Dtsch Med Wochenschr* 141: 1014-1018, 2016 (In German).
- Zheng R, Xie S, Lu X, Sun L, Zhou Y, Zhang Y and Wang K: A systematic review and meta-analysis of epidemiology and clinical manifestations of human brucellosis in China. *Biomed Res Int* 2018: 5712920, 2018.
- Galinska EM and Zagorski J: Brucellosis in humans-etiology, diagnostics, clinical forms. *Ann Agric Environ Med* 20: 233-238, 2013.
- Pelerito A, Cordeiro R, Matos R, Santos MA, Soeiro S, Santos J, Manita C, Rio C, Santo M, Paixão E, *et al*: Human brucellosis in portugal-retrospective analysis of suspected clinical cases of infection from 2009 to 2016. *PLoS One* 12: e0179667, 2017.
- Elfaki MG, Alaidan AA and Al-Hokail AA: Host response to brucella infection: Review and future perspective. *J Infect Dev Ctries* 9: 697-701, 2015.
- Miller CN, Smith EP, Cundiff JA, Knodler LA, Bailey Blackburn J, Lupashin V and Celli J: A brucella type iv effector targets the cog tethering complex to remodel host secretory traffic and promote intracellular replication. *Cell Host Microbe* 22: 317-329, 2017.
- Carvalho TF, Haddad JP, Paixão TA and Santos RL: Meta-Analysis and advancement of brucellosis vaccinology. *PLoS One* 11: e0166582, 2016.
- Schaaf K, Smith SR, Duverger A, Wagner F, Wolschendorf F, Westfall AO, Kutsch O and Sun J: *Mycobacterium tuberculosis* exploits the PPM1A signaling pathway to block host macrophage apoptosis. *Sci Rep* 7: 42101, 2017.
- Sun J, Schaaf K, Duverger A, Wolschendorf F, Speer A, Wagner F, Niederweis M and Kutsch O: Protein phosphatase, Mg<sup>2+</sup>/Mn<sup>2+</sup>-dependent 1A controls the innate antiviral and antibacterial response of macrophages during HIV-1 and *mycobacterium tuberculosis* infection. *Oncotarget* 7: 15394-15409, 2016.
- Xiang W, Zhang Q, Lin X, Wu S, Zhou Y, Meng F, Fan Y, Shen T, Xiao M, Xia Z, *et al*: PPM1A silences cytosolic RNA sensing and antiviral defense through direct dephosphorylation of MAVS and TBK1. *Sci Adv* 2: e1501889, 2016.
- Siqueira MDS, Ribeiro RM and Travassos LH: Autophagy and its interaction with intracellular bacterial pathogens. *Front Immunol* 9: 935, 2018.
- Li Y, Wei C, Xu H, Jia J, Wei Z, Guo R, Jia Y, Wu Y, Li Y, Qi X, *et al*: The immunoregulation of Th17 in host against intracellular bacterial infection. *Mediators Inflamm* 19: 6587296, 2018.
- Heppner FL, Ransohoff RM and Becher B: Immune attack: The role of inflammation in alzheimer disease. *Nat Rev Neurosci* 16: 358-372, 2015.
- Yang J, Zhang J, Xu T, Wang Y and Wang Z: Establishment of BV2 cell line with steady knockdown of Mg<sup>2+</sup>/Mn<sup>2+</sup>-dependent protein phosphatase 1A (PPM1A). *Xi Bao Yu Fen Zi Mian Yi Xue Za Zhi* 34: 818-823, 2018 (In Chinese).
- Ma QL, Liu AC, Ma XJ, Wang YB, Hou YT and Wang ZH: Brucella outer membrane protein Omp25 induces microglial cells in vitro to secrete inflammatory cytokines and inhibit apoptosis. *Int J Clin Exp Med* 8: 17530-17535, 2015.
- Smith SR, Schaaf K, Rajabalee N, Wagner F, Duverger A, Kutsch O and Sun J: The phosphatase PPM1A controls monocyte-to-macrophage differentiation. *Sci Rep* 8: 902, 2018.
- Wang Y, Dow EC, Liang YY, Ramakrishnan R, Liu H, Sung TL, Lin X and Rice AP: Phosphatase PPM1A regulates phosphorylation of thr-186 in the Cdk9 T-loop. *J Biol Chem* 283: 33578-33584, 2008.
- Sun W, Yu Y, Dotti G, Shen T, Tan X, Savoldo B, Pass AK, Chu M, Zhang D, Lu X, *et al*: PPM1A and PPM1B act as IKKbeta phosphatases to terminate TNFalpha-induced IKKbeta-NF-kappaB activation. *Cell Signal* 21: 95-102, 2009.
- Levy J, Shneck M, Marcus M and Lifshitz T: Brucella meningitis and papilledema in a child. *Eur J Ophthalmol* 15: 818-820, 2005.
- Haji-Abdolbagi M, Rasooli-Nejad M, Jafari S, Hasibi M and Soudbakhsh A: Clinical and laboratory findings in neurobrucellosis: Review of 31 cases. *Arch Iran Med* 11: 21-25, 2008.
- Li YJ, Li XL, Liang S, Fang LQ and Cao WC: Epidemiological features and risk factors associated with the spatial and temporal distribution of human brucellosis in China. *BMC Infect Dis* 13: 547, 2013.
- Lai S, Zhou H, Xiong W, Gilbert M, Huang Z, Yu J, Yin W, Wang L, Chen Q, Li Y, *et al*: Changing epidemiology of human brucellosis, China, 1955-2014. *Emerg Infect Dis* 23: 184-194, 2017.
- Deng Y, Liu X, Duan K and Peng Q: Research progress on brucellosis. *Curr Med Chem* 26: 5598-5608, 2018.
- Tu L, Liu X, Gu W, Wang Z, Zhang E, Kahar A, Chu G and Zhao J: Imaging-assisted diagnosis and characteristics of suspected spinal brucellosis: A retrospective study of 72 cases. *Med Sci Monit* 24: 2647-2654, 2018.
- Sabzi F and Faraji R: Brucella pericarditis: A forgotten cause of chest pain. *Caspian J Intern Med* 8: 116-118, 2017.
- Olsen SC and Palmer MV: Advancement of knowledge of brucella over the past 50 years. *Vet Pathol* 51: 1076-1089, 2014.
- Moreno E and Moriyon I: Brucella melitensis: A nasty bug with hidden credentials for virulence. *Proc Natl Acad Sci USA* 99: 1-3, 2002.



This work is licensed under a Creative Commons Attribution-NonCommercial-NoDerivatives 4.0 International (CC BY-NC-ND 4.0) License.